DISEASES AND DISORDERS

LSD1 enzyme inhibitor TAK-418 unlocks aberrant epigenetic machinery and improves autism symptoms in neurodevelopmental disorder models

Rina Baba[1]*, Satoru Matsuda[1]*, Yuuichi Arakawa[1†], Ryuji Yamada[1], Noriko Suzuki[1†], Tatsuya Ando[2], Hideyuki Oki[3†], Shigeru Igaki[3], Masaki Daini[1], Yasushi Hattori[1], Shigemitsu Matsumoto[1‡], Mitsuhiro Ito[1†], Atsushi Nakatani[1], Haruhide Kimura[1§]

Persistent epigenetic dysregulation may underlie the pathophysiology of neurodevelopmental disorders, such as autism spectrum disorder (ASD). Here, we show that the inhibition of lysine-specific demethylase 1 (LSD1) enzyme activity normalizes aberrant epigenetic control of gene expression in neurodevelopmental disorders. Maternal exposure to valproate or poly I:C caused sustained dysregulation of gene expression in the brain and ASD-like social and cognitive deficits after birth in rodents. Unexpectedly, a specific inhibitor of LSD1 enzyme activity, 5-((1*R*,2*R*)-2-((cyclopropylmethyl)amino)cyclopropyl)-*N*-(tetrahydro-2*H*-pyran-4-yl)thiophene-3-carboxamide hydrochloride (TAK-418), almost completely normalized the dysregulated gene expression in the brain and ameliorated some ASD-like behaviors in these models. The genes modulated by TAK-418 were almost completely different across the models and their ages. These results suggest that LSD1 enzyme activity may stabilize the aberrant epigenetic machinery in neurodevelopmental disorders, and the inhibition of LSD1 enzyme activity may be the master key to recover gene expression homeostasis. TAK-418 may benefit patients with neurodevelopmental disorders.

INTRODUCTION

Epigenetic dysregulation may be associated with the pathophysiology of neurodevelopmental disorders. For example, several de novo mutations in the genes encoding epigenetic modulators such as *CHD8* and *KMT2C* have been identified in individuals with autism spectrum disorder (ASD) (*1*). In addition, environmental insults during early life may be related to their etiology through persistent epigenetic dysregulation. For example, prenatal exposure to valproate (VPA), a histone deacetylase inhibitor, increases ASD risk (*2*). Prenatal viral infection is associated with increased risk of ASD and schizophrenia (*3*). Neuroinflammation caused by prenatal viral infection (*4*) or altered microbiota is also considered an environmental risk factor for ASD (*5*). Furthermore, a discordance in ASD diagnosis is observed within monozygotic twin pairs (with identical DNA sequences) (*6*, *7*). Therefore, environmental impacts can cause neurodevelopmental disorders with lifelong disabilities through sustained epigenetic dysfunction.

Clarification of the mechanisms underlying the persistent pathogenic changes in epigenetic machinery is essential for developing novel therapies for neurodevelopmental disorders. Dysregulation of histone H3 lysine 4 (H3K4) methylation is closely associated with neurodevelopmental disorders, including ASD (*8*, *9*). We focused on LSD1, which demethylates mono- and dimethylated H3K4 (H3K4me1/2) and histone H3 lysine 9 (H3K9me1/2) (*10*, *11*). LSD1 has been considered to regulate gene expression through two functions: histone demethylation and scaffolding activity for cofactors, including growth factor independent 1B (GFI1B), a critical regulator of hematopoietic differentiation (*12*, *13*). In the previous study, characterization of two LSD1 inhibitors [*N*-(4-(*trans*-2-((cyclopropylmethyl)amino)cyclopropyl)phenyl) biphenyl-4-carboxamide hydrochloride (T-711) and 3-((1*S*,2*R*)-2-(cyclobutylamino)cyclopropyl)-*N*-(5-methyl-1,3,4-thiadiazol-2-yl) benzamide fumarate (T-448)] revealed that T-711 modulates both of these functions and causes thrombocytopenia, while T-448 selectively inhibits histone demethylation with low hematological toxicity (*13*).

Here, we identify a novel T-448–type LSD1inhibitor, 5-((1*R*,2*R*)-2-((cyclopropylmethyl)amino)cyclopropyl)-*N*-(tetrahydro-2*H*-pyran-4-yl)thiophene-3-carboxamide hydrochloride (TAK-418) as a clinical candidate (ClinicalTrials.gov identifiers: NCT03228433 and NCT03501069). We found that inhibition of LSD1 enzyme activity by TAK-418 almost completely normalized the dysregulated gene expression levels in the brain and ameliorated ASD-like behavioral abnormalities in various rodent models of neurodevelopmental disorders with prenatal impacts. TAK-418 modulated almost completely different sets of genes across the models and their ages. TAK-418 also normalized aberrant epigenetic modifications such as DNA methylation in these models. These results suggest that the environmental insults during early life may cause sustained epigenetic dysregulation and aberrant gene expression and that LSD1 inhibition by TAK-418 may unlock the epigenetic machinery that stabilizes aberrant gene expression. TAK-418 could be a potential therapeutic agent for neurodevelopmental disorders through normalization of dysregulated global gene expression.

RESULTS

TAK-418 is a specific inhibitor of LSD1 enzyme activity

TAK-418 selectively inhibited LSD1 enzyme activity with a median inhibitory concentration (IC_{50}) value of 2.9 nM and with a k_{inact}/K_I

[1]Neuroscience Drug Discovery Unit, Research, Takeda Pharmaceutical Company Limited 26-1, Muraoka-Higashi 2-chome, Fujisawa, Kanagawa 251-8555, Japan. [2]Computational Biology, Research, Takeda Pharmaceutical Company Limited 26-1, Muraoka-Higashi 2-chome, Fujisawa, Kanagawa 251-8555, Japan. [3]Biomolecular Research Laboratories, Research, Takeda Pharmaceutical Company Limited 26-1, Muraoka-Higashi 2-chome, Fujisawa, Kanagawa 251-8555, Japan.
*These authors contributed equally to this work.
†Present address: Axcelead Drug Discovery Partners Inc. 26-1, Muraoka-Higashi 2-chome, Fujisawa, Kanagawa 251-0012, Japan.
‡Present address: SCOHIA PHARMA, Inc. 26-1, Muraoka-Higashi 2-chome, Fujisawa, Kanagawa 251-8555, Japan.
§Corresponding author. Email: haruhide.kimura@takeda.com

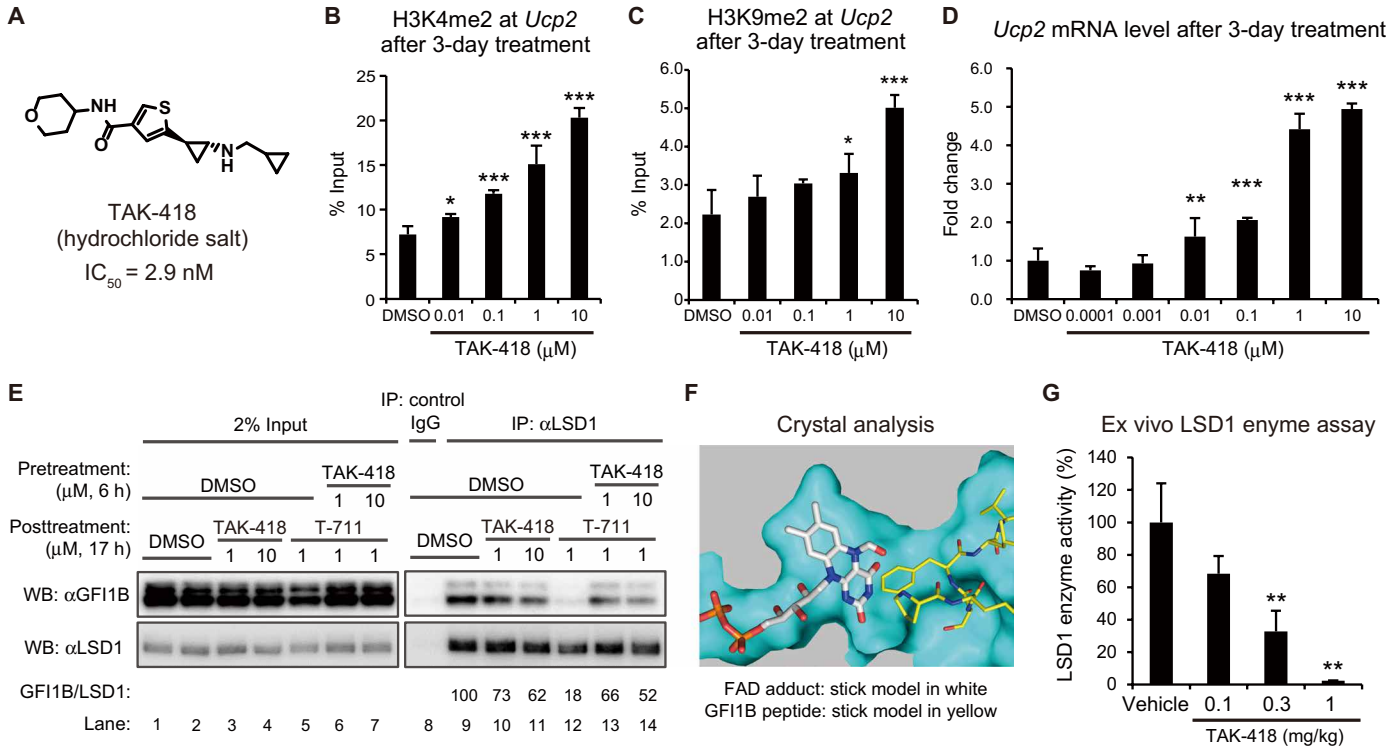

Fig. 1. TAK-418 is a specific inhibitor of LSD1 enzyme activity. (**A**) Chemical structure of TAK-418. (**B** to **D**) Effects of 3-day TAK-418 treatment on H3K4me2 (B) and H3K9me2 (C) levels at the *Ucp2* gene and *Ucp2* mRNA levels (D) in primary cultured rat neurons. $N = 3$ to 4. One-tailed parametric Williams' test versus DMSO-treated groups, $^{*}P < 0.025$, $^{**}P < 0.005$, and $^{***}P < 0.0005$. (**E**) Immunoprecipitation (IP) analyses of the interaction between LSD1 and GFI1B in TF-1a cells. GFI1B/LSD1 values are obtained from densitometry data of GFI1B bands normalized by LSD1 bands (lane 9 = 100%). IgG, immunoglobulin G; WB, Western blotting. (**F**) Superimposed structure of formylated FAD (stick model in white) in human recombinant LSD1 generated after TAK-418 treatment and N-terminal GFI1B peptide (PRSFLV, stick model in yellow) in the LSD1 complex. The formyl-FAD adduct is compact in the active site of LSD1 and has minimal impact on the interaction between LSD1 and GFI1B. (**G**) Dose-dependent change in LSD1 enzyme activity in the rat cortex 2 hours after administration of TAK-418. $N = 3$ to 6. One-tailed Shirley-Williams test versus vehicle-treated group, $^{**}P < 0.005$. Data are shown as means + SD.

value of $3.8 \times 10^5 \pm 3.8 \times 10^4$ (M^{-1} s^{-1}) (Fig. 1A, fig. S1, A to D, and table S1). We have previously found that LSD1 inhibition could increase histone methylation at *Ucp2* and *Bdnf* genes (*13*). Thus, histone methylation levels of these genes were used as markers for LSD1 inhibition by TAK-418. TAK-418 increased H3K4me1/2/3 and H3K9me2 levels at the *Ucp2* gene (Fig. 1, B and C, and fig. S1, E to G) and induced *Ucp2* mRNA expression in primary cultured rat neurons (Fig. 1D). TAK-418 also increased H3K4me1/2/3 at the *Bdnf* gene (fig. S1, H to J). Different from T-711 and similar to T-448, TAK-418 had minimal impact on the interaction between LSD1 and its cofactor, GFI1B (Fig. 1E and fig. S1, K to M); TAK-418 avoided the steric interference with GFI1B in the binding pocket through the generation of a compact formylated adduct form of coenzyme flavin adenine dinucleotide (FAD) (Fig. 1F and fig. S1N). TAK-418 showed a good pharmacokinetic profile in rodents (fig. S2, A to H) and inhibited LSD1 enzyme activity in the brain (Fig. 1G and fig. S2, I to K) without causing hematological toxicity in rodents (fig. S2, L and M). Single administration of TAK-418 at 1 or 3 mg/kg increased H3K4me2 levels at *Ucp2* gene in the mouse brain (fig. S2N). The discovery of TAK-418 enabled us to specifically characterize the biological functions of LSD1 enzyme activity without being interfered by the LSD1-cofactor complex-derived signals.

TAK-418 normalizes mRNA expression dysregulated in neurodevelopmental disorder model rodents

To characterize the effects of TAK-418 on the persistent pathogenic changes in epigenetic machinery, we used animal models of neurodevelopmental disorders that satisfied the following two criteria: (i) mimicking the prenatal environmental impacts involved in disease etiology in humans and (ii) expressing sustained ASD-like symptoms. Rats with maternal exposure to VPA (VPA rats) (*14*, *15*) and mice with maternal exposure to polyinosinic:polycytidylic acid (poly I:C), a mimetic of prenatal viral infection (poly I:C mice) (*16*), satisfied these criteria. Oral administration of TAK-418 at 1 mg/kg showed 91.5 and 95.7% inhibition of LSD1 enzyme activity in mice and VPA rats, respectively (fig. S2, J and O). To ensure that poly I:C mice are reproducible, poly I:C lot-to-lot variability in the context of the induction of maternal immune responses should be carefully monitored (*17*). Notably, the poly I:C used in this study induced potent cytokine production in maternal plasma (fig. S3). To globally analyze the effects of TAK-418 (1 mg/kg) on mRNA expression in these animal models, RNA sequencing (RNA-seq) was performed using cortical tissues isolated from juvenile VPA rats (5-week-old), adult VPA rats (15-week-old), and adult poly I:C mice (22-week-old), 1 day after a 2-week once daily (QD) administration of TAK-418. The volcano plots (fig. S4, A to C) show the overall changes in mRNA

expression in the model animals compared to the corresponding control animals and the overall changes in mRNA expression with TAK-418 treatment. To assess the impact of TAK-418 on the dysregulated gene expression in each model, gene set enrichment analysis (GSEA) was performed by using the top 100 dysregulated (up-regulated and down-regulated) genes with low false discovery rates (FDRs) in each model (Fig. 2, A to C). The GSEA plots of the dysregulated genes in the ranked list of genes modified by TAK-418 revealed that expression of both up- and down-regulated genes in all animal models was substantially counteracted by TAK-418. In other words, inverse correlations between the changes in the models and the effects of TAK-418 were observed in all tested models.

To further evaluate the normalizing effects of TAK-418 on gene expression from the perspective of not only the direction of the expression changes but also the magnitude of the expression changes, we decided to focus on the genes with significant changes in the model animals and those with significant changes after TAK-418 treatment. First, differentially expressed genes (DEGs) were identified using the criterion of FDR < 0.2. The numbers of DEGs in the disease models (disease-DEGs) and DEGs with TAK-418 (TAK-418–DEGs) are summarized in fig. S4D. The $\log_2$ fold change (FC) values of both disease-DEGs and TAK-418–DEGs are plotted in fig. S4E; however, there were few dual DEGs (defined as being both a disease-DEG and TAK-418–DEG) in any of the models (two dual DEGs in

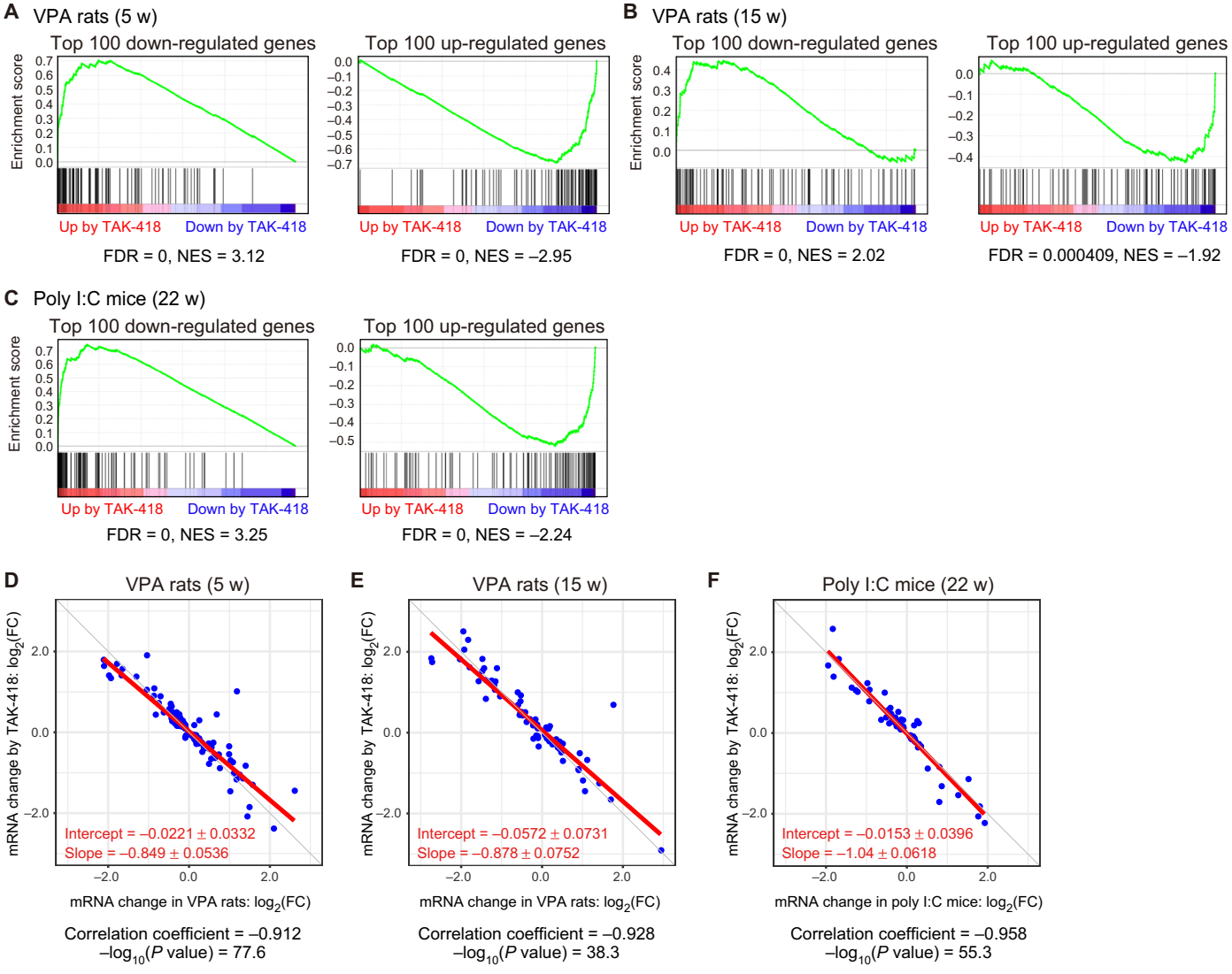

Fig. 2. TAK-418 normalizes mRNA expression dysregulated in VPA rats and poly I:C mice. (**A** to **C**) GSEA plots for the top 100 dysregulated (down-regulated/up-regulated) genes with low *q* values in 5-week-old (A) and 15-week-old (B) VPA rats and 22-week-old poly I:C mice (C) in the ranked list of genes modified by TAK-418 (red, up-regulation by TAK-418; blue, down-regulation by TAK-418). The green curves correspond to the enrichment score curves: The running sums of the weighted enrichment score obtained from GSEA software. Normalized enrichment score (NES) and corresponding FDR values are shown in each panel. (**D** to **F**) Scatter plots and Pearson's correlation analysis between mRNA expression alteration patterns and the effects of TAK-418 on mRNA expression in 5-week-old (D) and 15-week-old VPA rats (E) and 22-week-old poly I:C mice (F). *x* axis, FC values of mRNA expression levels in disease model animals relative to those in control animal; *y* axis, FC values of mRNA expression levels in TAK-418–treated disease model animals relative to vehicle-treated model animals. Fitted regression lines and their slopes and intercepts with 95% confidence intervals are shown in red.

the 5-week-old VPA rats, no dual DEGs in the 15-week-old VPA rats, and one dual DEG in the poly I:C mice). Thus, we decided to use the genes with expression levels that were dysregulated in each animal model ($P < 0.05$, without multiple comparison correction) and modulated by TAK-418 treatment ($P < 0.05$, without multiple comparison correction). Unexpectedly, a strong inverse correlation was observed in each animal model, with correlation coefficient values of −0.912 in juvenile VPA rats (Fig. 2D), −0.928 in adult VPA rats (Fig. 2E), and −0.958 in adult poly I:C mice (Fig. 2F). Moreover, the fitted regression lines were almost described by the equation $y = -x$. Figure S4F depicts the differential expression levels in the vehicle- or TAK-418–treated disease models where the control level was normalized to 100%; gene expression was almost completely normalized by TAK-418 in both the direction and magnitude of change, irrespective of the disease model or animal age. When assessing all disease-DEGs (identified as FDR < 0.2) within each disease model, most of these disease-DEGs (62.3% in juvenile VPA rats and 60.0% in adult poly I:C mice) were no longer dysregulated after treatment with TAK-418 (fig. S4G). In the 15-week-old VPA rats, only 33.9% of the disease-DEGs were no longer dysregulated after TAK-418 treatment. This result suggests that the effects of TAK-418 on the normalization of gene expression were more robust in the 5-week-old VPA rats than in the 15-week-old VPA rats. Therefore, TAK-418 counteracted both the direction and magnitude of dysregulated gene expression in each neurodevelopmental disorder model. The hierarchical clustering of the mRNA expression profile in the control animals, vehicle-treated model animals, and TAK-418–treated model animals revealed that the control animals and TAK-418–treated model animals were segregated from the vehicle-treated model animal group, as observed by the separation of the samples into two clusters based on the tree cut in 5-week-old VPA rats and in poly I:C mice but not in 15-week-old VPA rats (fig. S5). It must be noted that normal gene expression may not have occurred in these animal models after birth.

TAK-418 may recover homeostatic regulation of global gene expression

To understand the mechanism underlying TAK-418 function in normalizing dysregulated gene expression, we explored the common disease-DEGs across the three models. Overlapping analysis revealed that dysregulated patterns of mRNA expression in the brain were almost completely different between these animal models (Fig. 3A). In addition, the biological/functional pathways with significant ($q < 0.2$) enrichment in the disease-DEGs showed no overlaps (Fig. 3B). The top 10 pathways based on normalized enrichment scores (NESs) in each model are shown in fig. S6 (A to C).

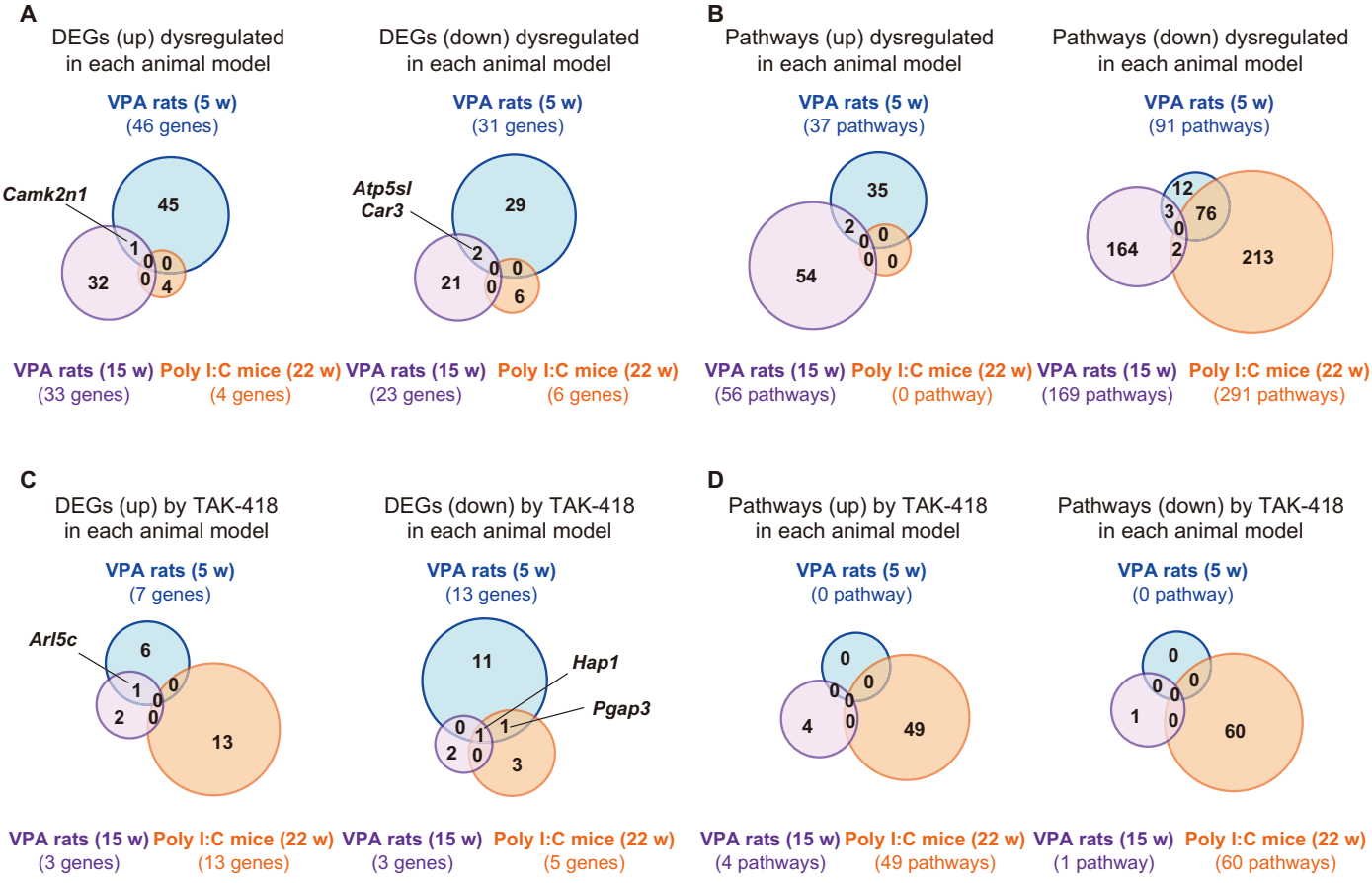

Fig. 3. TAK-418 modulates completely different gene sets to normalize gene expression in VPA rats and poly I:C mice. (**A** and **B**) Venn diagrams showing overlap among the up-/down-regulated disease-DEGs in the disease model animals (A) and overlap among the biological pathways significantly enriched (q value < 0.2) in the up-/down-regulated disease-DEGs (B). (**C** and **D**) Venn diagrams showing overlap among the up-/down-regulated TAK-418–DEGs in the model animals (C) and overlap across the biological pathways significantly enriched (q value < 0.2) in the up-/down-regulated TAK-418–DEGs in the model animals (D).

Next, we explored the common TAK-418–DEGs. However, *Hap1* (*Huntingtin-associated protein 1*) was the only common TAK-418–DEG across the models (Fig. 3C), and thus, it was difficult to explain the mechanism underlying the global gene normalization by TAK-418. In addition, there were no overlaps in the pathways significantly modulated by TAK-418 ($q < 0.2$) across the three models (Fig. 3D and fig. S6, D to F). These results seem reasonable because the TAK-418–DEGs were scarcely overlapped across the models (Fig. 3C). Therefore, even if the dysregulated patterns of gene expression in each disease model are different, TAK-418 could precisely counteract the dysregulated expression both in direction and magnitude. TAK-418 may recover homeostatic regulation of global gene expression in responding to each disease state rather than through the modification of specific genes or pathways.

TAK-418 normalizes DNA methylation dysregulated in VPA rats and poly I:C mice

To further investigate the effects of TAK-418 on epigenetic modifications such as histone acetylation/methylation and DNA methylation, chromatin immunoprecipitation sequencing (ChIP-seq) and reduced representation bisulfite sequencing (RRBS) were performed by using the brains isolated from juvenile VPA rats and adult poly I:C mice the day after the 2-week treatment with vehicle or TAK-418. For histone modification, genomic regions within ±7500 bp from transcription start site (TSS) were analyzed. For DNA methylation, genomic regions within −2000 bp from TSS were analyzed. In the VPA rats, H3K4me3, H3K9ac, and H3K9me3 levels were increased (fig. S7, A to C). There were no notable changes in the H3K27me3 level (fig. S7D). DNA methylation levels were dysregulated both in up- and down-regulation manners (fig. S7E). There was an overall tendency of decrease in H3K9ac levels with TAK-418 treatment, counteracting the changes in 5-week-old VPA rats (fig. S7B). Differentially modulated genomic regions (DMGs) in the 5-week-old VPA rats [VPA(5w)-DMGs] were identified using the criterion of FDR < 0.2, and the DMG numbers are shown in fig. S7F. Almost all of the VPA(5w)-DMGs involved increased H3K9ac and H3K9me3 levels, and none of the VPA(5w)-DMGs were dysregulated after TAK-418 treatment (fig. S7G). FC plot analysis between the changes in the VPA rats and the effects of TAK-418 (fig. S7, H and I) for these DMGs suggested that strong and weak inverse correlations existed for H3K9ac and H3K9me3, respectively. In the poly I:C mice, H3K4me3 and H3K9ac levels showed a tendency to decrease (fig. S7, J and K). There were no notable changes in H3K9me3 or H3K27me3 levels (fig. S7, L and M). DNA methylation levels were both increased and decreased (fig. S7N). There were only a few DMGs (FDR < 0.2) in the poly I:C mice (fig. S7O); thus, FC plot analyses using DMGs could not be conducted.

To assess further the normalizing effects of TAK-418 by focusing more on the magnitude of epigenetic dysregulation in these model animals, we used the genomic regions that had dysregulated epigenetic modifications ($P < 0.05$, without multiple comparison correction) and were also modulated by TAK-418 treatment ($P < 0.05$, without multiple comparison correction). In the VPA rats, the plots for FC values in H3K9ac levels showed a clear negative correlation (correlation coefficient = −0.75) (Fig. 4A). There were only 12 regions with significant H3K4me3 changes by TAK-418 (Fig. 4B). The plots for the differences in DNA methylation levels showed a clear negative correlation (correlation coefficient = −0.90) (Fig. 4C). There were no regions with significant H3K9me3 or H3K27me3 changes by TAK-418. These results suggested that TAK-418 normalized the dysregulated patterns of H3K9ac and DNA methylation in the VPA rats. In the poly I:C mice, a strong inverse correlation was observed in DNA methylation levels with a correlation coefficient value of −0.96 (Fig. 4D). There were no regions with significant modifications on histone marks. These results suggest that TAK-418 normalized the dysregulated patterns of DNA methylation in the poly I:C mice. In both the VPA rats and poly I:C mice, DNA methylation was normalized with fitted regression lines of almost $y = -x$ (Fig. 4, C and D). Thus, although the patterns of epigenetic dysregulation are different across the models, TAK-418 normalized gene expression and DNA methylation in both models.

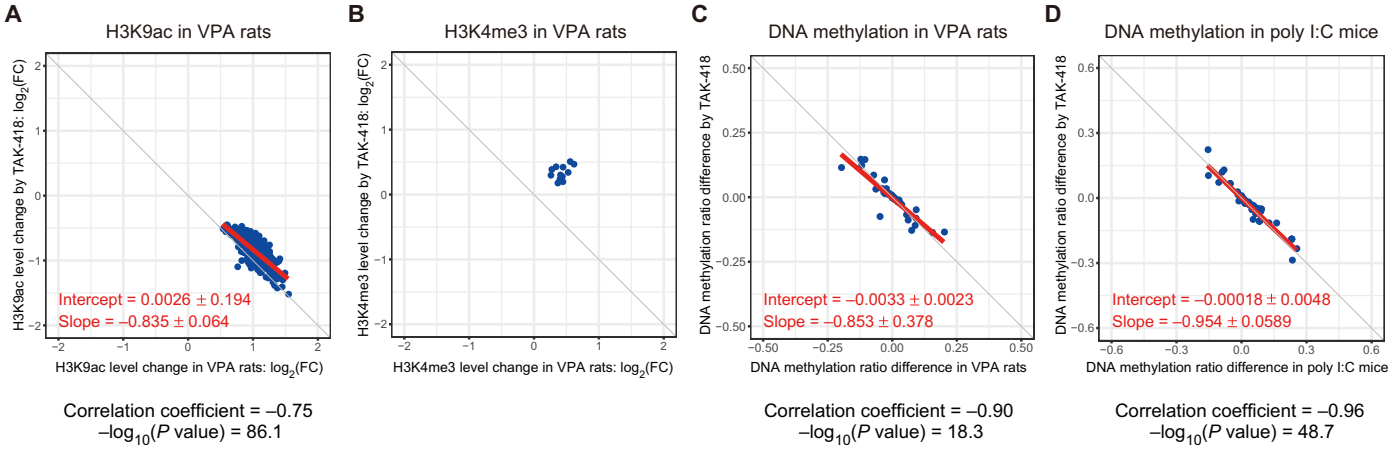

Fig. 4. TAK-418 produces inverse correlation against the histone modification and DNA methylation levels altered in VPA rats and poly I:C mice. (**A** to **C**) Scatter plots and Pearson's correlation analyses between alteration patterns of H3K9ac (A), H3K4me3 (B), and DNA methylation (C) and the effects of TAK-418 in VPA rats. (**D**) Scatter plots and Pearson's correlation analyses between alteration patterns of DNA methylation and effects of TAK-418 in poly I:C mice. *x* axis, FC values of histone modification levels or difference in DNA methylation ratio in model animals, compared to those in control animals; *y* axis, FC values of histone modification levels or difference in DNA methylation ratio in TAK-418–treated model animals, compared to those in vehicle-treated model animals. Fitted regression lines and their slopes and intercepts with 95% confidence intervals are shown in red.

The epigenetic profile around the genomic regions of the disease-DEGs and TAK-418–DEGs was obtained from the ChIP-seq and RRBS analysis data (tables S2 and S3, respectively). From this snapshot assessment, expression changes of individual DEGs were not correlated with their status of epigenetic modification. The dynamics of epigenetic and gene expression modulation may follow different time courses.

TAK-418 ameliorates some ASD-like behaviors in neurodevelopmental disorder model rodents

Next, we asked whether the persistent ASD-like behavioral deficits can be improved by TAK-418 treatment. Two-week QD administration of TAK-418 (1 mg/kg) to juvenile and adult VPA rats completely recovered their sociability, as indicated by the sniffing index (Fig. 5, A and B). TAK-418 at 0.1 or 0.3 mg/kg was not significantly effective in juvenile VPA rats (Fig. 5A). Moreover, 2-week QD administration of TAK-418 (0.1, 0.3, or 1 mg/kg) to adult poly I:C mice significantly increased the sniffing index (Fig. 5, C to E). The rescuing effect of TAK-418 on the sniffing index diminished after the 1-week withdrawal period (Fig. 5F). One-week QD administration of TAK-418 (1 mg/kg) to juvenile VPA rats also recovered their sociability (Fig. 5G); however, single administration of TAK-418 was not effective in juvenile VPA rats (Fig. 5H). Thus, repeated TAK-418 treatment may ameliorate sociability deficits caused by prenatal perturbation of neurodevelopment.

The effects of TAK-418 on cognitive function were evaluated by novel object recognition (NOR) tests in juvenile VPA rats. QD administration of TAK-418 (1 mg/kg) for 16 to 20 days significantly rescued the decreased novelty discrimination index (NDI), an indicator of cognition, in the VPA rats (Fig. 6A). TAK-418 (1 mg/kg, single or 2-week QD administration) had no effects on delay-dependent forgetting of object memory in NOR tests in age-matched normal rats (Fig. 6B). TAK-418 may exert its therapeutic effects by normalizing pathological gene expression.

Juvenile VPA rats showed a tendency for increased repetitive behaviors in open field tests, which were tended to be ameliorated upon TAK-418 treatment (fig. S8A). We also attempted to assess the repetitive behaviors in VPA rats by Y-maze tests; however, there were no changes in spontaneous alternation activity ratios or alternation scores (fig. S8B), making it difficult to evaluate the effects of TAK-418. Further evaluation using animal models with various ASD-like symptoms would be valuable.

DISCUSSION

There is a huge unmet need for novel therapies with improved efficacy for neurodevelopmental disorders such as ASD and schizophrenia. However, critical players for the pathogenic machinery for these disorders remain unknown. In this study, we found that the inhibition of LSD1 enzyme activity by TAK-418 recovered gene expression homeostasis (normalization of gene expression both in magnitude and direction) in the brain of two rodent models of neurodevelopmental disorders and ameliorated some ASD-like behaviors in these animals. The genes and biological pathways modulated by TAK-418 were almost completely different across the models and their ages. In both the VPA rats and poly I:C mice, TAK-418 globally normalized the magnitude and direction of DNA methylation. Considering the hypothesis that long-term changes in genome-wide DNA methylation are the hallmarks of prenatal pathogenic impacts on neurodevelopment (*18*), the normalization of DNA methylation could be the intermediate status involved in the therapeutic mechanism of action of TAK-418. LSD1 is known to demethylate DNMT1 (DNA methyl-transferase 1) and enhance its protein stability (*19*); however, this function does not fully explain the normalization in DNA methylation because DNA methylation levels were both increased and decreased in the model animals. These results cannot be explained by the currently known biological function of LSD1 (the control of histone H3K4/H3K9 methylation levels), and they imply previously unknown function of LSD1 in the control of global gene transcription. Our hypothesis is illustrated in fig. S9; TAK-418 first increases H3K4me and H3K9me, and these changes trigger subsequent changes in epigenetic cross-talk beyond H3K4 and H3K9 methylation, resulting in the normalization of DNA methylation and gene expression. The modulations of H3K4me and H3K9me are associated with activated and silenced transcription, respectively; thus, LSD1 has double-sided effects on gene expression. As negative feedbacks are widely used to maintain homeostasis, the impacts of H3K4me can be greater for down-regulated genes than for up-regulated genes, and the impact of H3K9me can be greater for the up-regulated genes than for down-regulated genes in model animals. In addition, prolonged treatment with TAK-418 may have broader impacts on the epigenetic cross-talk mechanism beyond H3K4 and H3K9 methylation. For example, chronic TAK-418 treatment altered the expression of *Klf10* [known to increase the expression of the histone lysine demethylase KDM6A (lysine demethylase 6A) (*20*)] and *Sgk1* [known to phosphorylate and suppress the activity of the lysine methyltransferase KMT2D (lysine methyltransferase 2D) (*21*)] in the 5-week-old VPA rats (table S3). During the 14-day TAK-418 treatment period, such epigenetic modifications would repeatedly and dynamically occur in multiple genes, responding to the expression status. Eventually, as observed in this study, gene expression would be normalized in a genome-wide manner. Further studies to clarify the mechanisms of action of TAK-418 including time course analysis to detect intermediate changes are needed.

TAK-418 showed similar efficacy for the improvement in sociability of juvenile (5-week-old) and adult (15-week-old) VPA rats (Fig. 5, A and B). To obtain further insight into the age-related differences in the effects of TAK-418, we compared the results of mRNA expression analysis between juvenile and adult VPA rats, because normalization of gene expression would be the pivotal mechanism underlying the therapeutic effect of TAK-418. There was no substantial difference in the strength of inverse correlation between the 5-week-old and in 15-week-old VPA rats (Fig. 2, D and E), and the fitted regression lines were almost described by the equation $y = -x$ in both ages. However, most of the VPA(5w)-DEGs (62.3%), but only 33.9% of the VPA(15w)-DEGs, were no longer dysregulated after TAK-418 treatment (fig. S4G). Clustering analyses also suggested that TAK-418 had stronger effects on the normalization of gene expression patterns in 5-week-old VPA rats than in 15-week-old VPA rats (fig. S5). Thus, the magnitude of dysregulated gene expression could be almost completely counteracted by TAK-418 irrespective of the animal age; however, a wider range of genes may be normalized by TAK-418 treatment in younger animals.

The biological/functional pathways enriched in the disease models suggest an age-dependent shift in the status of gene expression dysregulation in VPA rats (fig. S6). Immunological responses would be the main insults with poly I:C injection, as confirmed by the cytokine induction during the acute phase postinjection (fig. S3); however, immunological pathways were not identified in the lists shown

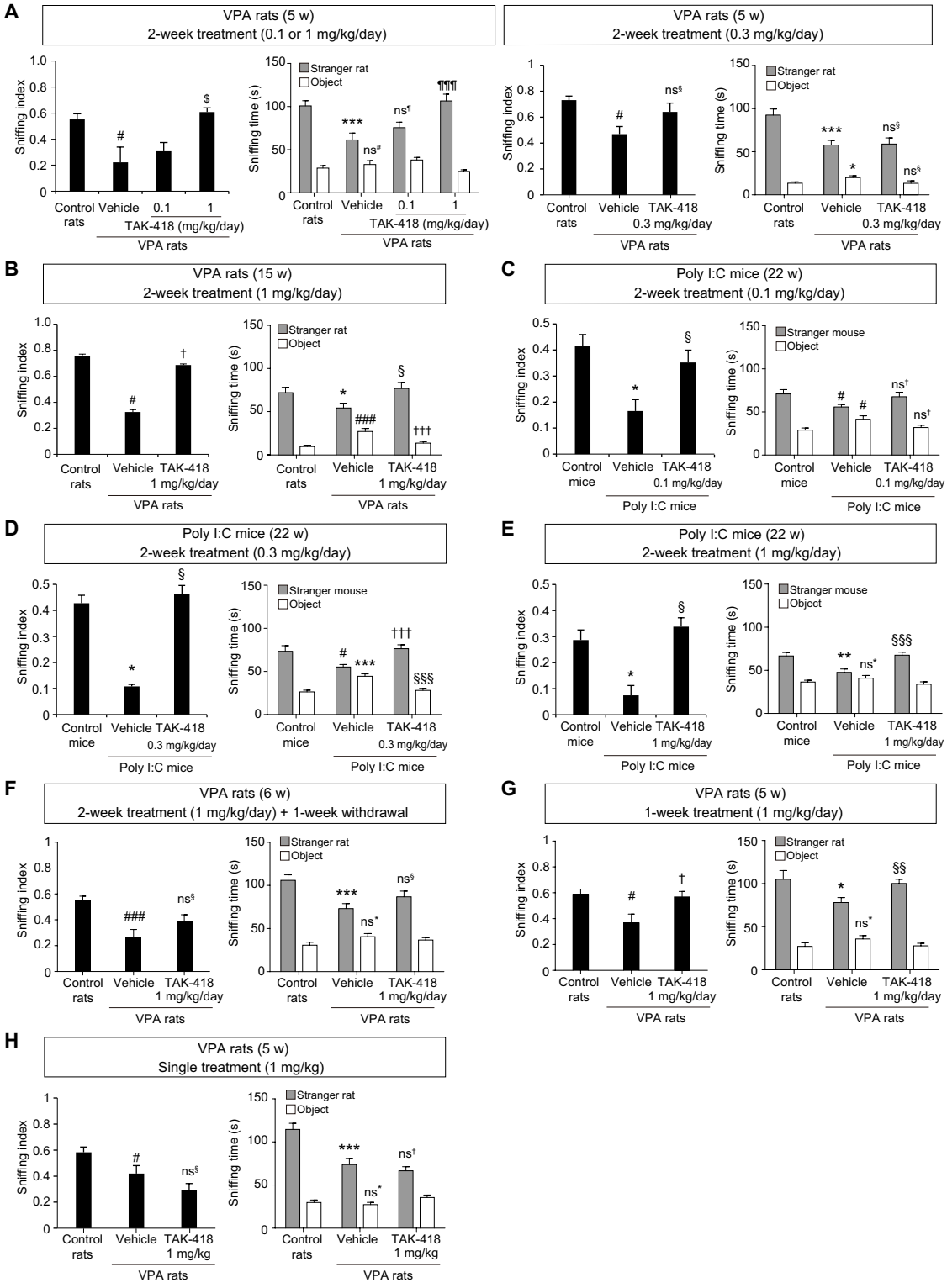

Fig. 5. TAK-418 ameliorates impaired sociability in VPA rats and poly I:C mice. (**A** and **B**) Effects of 2-week TAK-418 administration on social impairment in 5-week-old (A) and 15-week-old (B) VPA rats. $N = 14$ or 15. (**C** to **E**) Effects of 2-week TAK-418 administration at 0.1 (C), 0.3 (D), and 1 mg/kg (E) in 22-week-old poly I:C mice. $N = 13$ or 14. (**F**) Effects of 2-week TAK-418 administration in VPA rats assessed after 1-week drug withdrawal. $N = 14$ or 15. (**G**) Effects of 1-week TAK-418 administration in 5-week-old VPA rats. $N = 6$ or 10. (**H**) Effects of single TAK-418 administration in 5-week-old VPA rats. $N = 14$ or 15. All quantitative data are presented as means + SEM. Student's *t* test versus control group, $^{*}P < 0.05$, $^{**}P < 0.01$, and $^{***}P < 0.005$. Aspin-Welch test versus control group, $^{\#}P < 0.05$ and $^{\#\#\#}P < 0.005$. One-tailed Shirley-Williams test versus vehicle-treated model group, $^{\$}P < 0.025$. One-tailed Williams test versus vehicle-treated model group, $^{¶¶¶}P < 0.005$. Student's *t* test versus vehicle-treated model group, $^{\$}P < 0.05$, $^{\$\$}P < 0.01$, and $^{\$\$\$}P < 0.005$. Aspin-Welch test versus vehicle-treated model group, $^{\dagger}P < 0.05$ and $^{\dagger\dagger\dagger}P < 0.005$. ns, no significant difference by each statistical test.

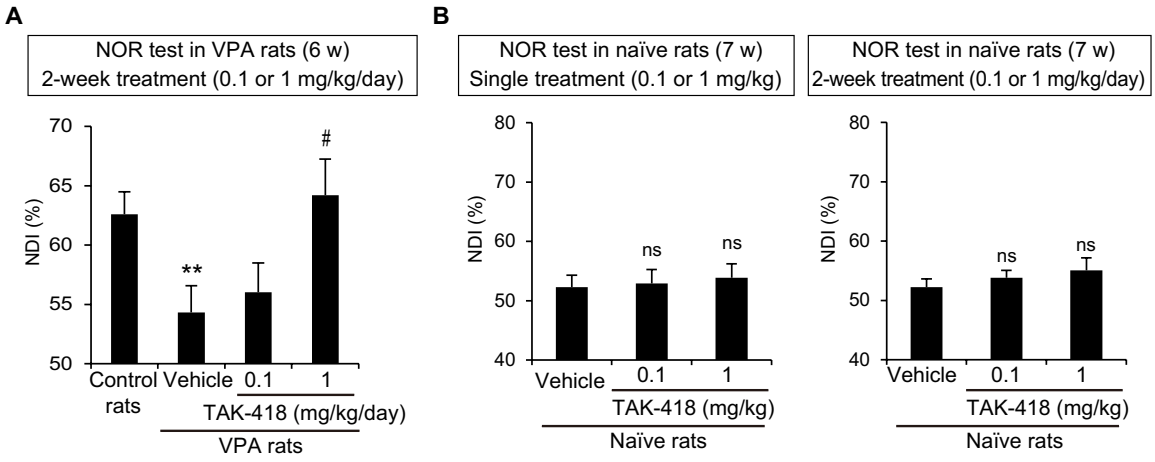

Fig. 6. TAK-418 ameliorates impaired cognitive function in VPA rats. (**A**) Effects of QD administration of TAK-418 for 16 to 20 days on cognitive deficit in VPA rats assessed by NOR tests. $N = 12$ to 15. Student's t test versus control rat group, $^{**}P < 0.01$. One-tailed Shirley-Williams test versus vehicle-treated VPA rats, $^{\#}P < 0.025$. (**B**) Effects of TAK-418 on cognition in naïve rats assessed by NOR tests. $N = 10$. ns, no significant difference by one-tailed Williams' test versus each vehicle-treated group. All quantitative data are presented as means + SEM.

in fig. S6C. These observations may be reasonable because age-dependent changes in gene expression and epigenetic modification patterns are known (*18*, *22*, *23*), and maternal cytokine induction by poly I:C injection is transient (*24*). Time-dependent changes in dysregulated biological/functional pathways may also be related to the phenotypic trait heterogeneity in neurodevelopmental disorders (*25*). Detailed mechanisms of action underlying these phenomena are not known; however, it could be related to the limited translatability of CNS drug development, because age-dependent changes and phenotypic variability in the preclinical efficacy of drugs have not been scrutinized. TAK-418 counteracted the dysregulated patterns of gene expression in both juvenile and adult VPA rats in this study. Moreover, TAK-418 ameliorated the behavioral deficits in the two models of neurodevelopmental disorders. Thus, we believe that TAK-418 has great therapeutic value.

The effects of TAK-418 on cognitive function were observed in VPA rats, but not in normal rats, implicating that TAK-418 exerts its therapeutic effects through normalization of dysregulated gene expression under pathological condition. Two-week QD administration of TAK-418 improved sociability in VPA rats, but the effect diminished after 1 week of drug withdrawal. A single administration of TAK-418 did not improve sociability in VPA rats. Further preclinical studies are needed to understand the therapeutic window of TAK-418 and the pathological conditions in which LSD1 inhibition by TAK-418 can normalize gene expression and improve behavioral disturbances. Moreover, clarification of underlying mechanisms of action for the recovery of gene expression homeostasis by TAK-418 would be needed. This information would contribute to the establishment of patient stratification strategy in early proof-of-concept studies.

Efficacy in preclinical ASD models is generally evaluated by not only sociability and cognitive functions but also other indexes such as repetitive behaviors (*15*). However, the abnormality in repetitive behaviors in the present study was not statistically significant (fig. S8); thus, it was difficult to reach a consensus about the effects of TAK-418 on other ASD-like symptoms. Studies using animal models with various behavioral and morphological ASD-like symptoms (*26*) would be beneficial to further understand the therapeutic potential of TAK-418 for ASD.

Experiments using animal models of neurodevelopmental disorders with prenatal manipulations require careful consideration of litter effects, pseudoreplication, and inflation of effect sizes (*27*–*30*). Detailed methods for generation of the model animals are described in Materials and Methods according to reporting guidelines (*30*), and the number of pups and dams for the generation of model animal is shown in table S4. Ideally, treated litters should be the experimental unit to mitigate these risks. However, considering the precious lives of experimental animals, we could not conduct all studies in meeting these criteria. In particular, a low number of litters (9 pups from two control dams and 18 pups from three VPA-treated dams used in the RNA-seq studies in 5-week-old VPA rats) should be considered as a limitation of this study. In Fig. 5G, one offspring per litter was used in each group, and the VPA rat pups were evenly allocated to vehicle-treated or TAK-418–treated group to balance the possible litter effects. As a result, we could detect the defects in sociability in the VPA rats and the improving effects of TAK-418 on the sociability. Therefore, the data we show here may have lower risks of litter effects, pseudoreplication, and inflation of effect sizes. It is also important to understand the effects of TAK-418 on gender, and thus, preclinical studies using female animals are required. The above-mentioned points are considered limitations of this TAK-418 study.

As discussed in a report using CHD8 haploinsufficient mice (*31*), an ASD model with epigenetic dysregulation may cause small but global changes in gene expression in the brain rather than prominent changes in specific genes. The condition of FDR < 0.2 or larger, but not widely used condition FDR < 0.05, has been used in some previously published studies (*18*, *32*); thus, we used FDR < 0.2 for the selection of DEGs. Further examination using other epigenetic-related disease models with larger gene expression changes followed by secondary analysis such as real-time polymerase chain reaction (PCR) is warranted.

It would be difficult to find the previously unknown functions of LSD1 enzyme activity shown here without using a unique LSD1 inhibitor such as TAK-418 because genetic ablation of LSD1 causes early embryonic lethality or severe thrombocytopenia (*19*, *33*), and the use of T-711–type conventional LSD1 inhibitors induces signals due to the LSD1-cofactor dissociation (*13*). TAK-418 may provide a unique opportunity to understand the regulation of the epigenetic

machinery in other developmental diseases such as childhood obesity caused by maternal diabetes (*34*).

MATERIALS AND METHODS

Study design

The objective of this study was to explore the effects of LSD1 enzyme inhibition by TAK-418 on persistent pathogenic changes in epigenetic machinery in neurodevelopmental disorders. For in vitro characterization of TAK-418, primary cultured rat neurons and TF-1a cells (human erythroblast cell line) were used. The sample size in these studies was determined on the basis of previous experience without a power analysis, and no data were excluded from the analysis. These experiments were repeated at least twice, and the experimental findings were reliably reproduced.

For in vivo characterization of TAK-418, ex vivo enzyme assay using tissues from rat or mice and in vivo blood cell number assay were performed. The sample size in these studies was determined on the basis of previous experience with similar animal studies without a power analysis, and no data were excluded from the analysis. These experiments were repeated at least twice with different dosing periods, and the experimental findings were reliably reproduced.

To examine the effects of TAK-418 in neurodevelopmental disorder model animals, we used VPA rats and poly I:C mice generated by the injection of VPA or poly I:C into pregnant rats or mice, respectively. For RNA-seq analysis, male VPA rats at 5 or 15 weeks old and male poly I:C mice at 22 weeks old were used. For ChIP-seq and RRBS analysis, male VPA rats at 5 weeks old and male poly I:C mice at 22 weeks old were used. These experiments were performed once with three replicated samples. For sociability test and cognition test, male VPA rats at 5, 6, or 15 weeks old and male poly I:C mice at 22 weeks old were used. The experiments were performed once in the exact same condition, but effects of TAK-418 were reproduced in the different conditions (different age at behavioral test in VPA rats or different dose of TAK-418 in poly I:C mice). The sample size in animal studies was determined on the basis of previous experience with similar animal studies. Animals were randomized into different groups with approximately comparable numbers of animals in each group. In the evaluation of sociability by sniffing test, subjects that did not sniff stranger animals or objects were removed from the analysis. In the evaluation of cognitive function by NOR test, subjects that spent less than 10 s of total exploration time during the acquisition trials were excluded. No data were excluded from the analysis in other tests. Behavior tests were performed under video recording, without blinding.

Animals

All experiments were approved by the Institutional Animal Care and Use Committee of Shonan Research Center, Takeda Pharmaceutical Company Limited. Male and pregnant Sprague-Dawley (SD) rats were purchased from Charles River Laboratories Japan Inc. Pregnant C57BL/6J mice were purchased from CLEA Japan Inc.

Chemicals

TAK-418 and T-711 were synthesized at the Medicinal Chemistry Research Laboratories, Takeda Pharmaceutical Company Limited or Fujimoto Chemicals Co. Ltd. TAK-418 was dissolved in dimethyl sulfoxide (DMSO) for in vitro experiments, distilled water containing 0.5% (w/v) methylcellulose and 0.5% (w/v) citrate for in vivo experiments with oral administration, or *N*,*N*-dimethylacetamide/polyethylene glycol 400 (1:1, v/v) for in vivo experiments with intravenous administration. The TAK-418 solution was administered to animals at dose volume of 1 ml/kg body weight (for rats and mice with intravenous administration), 2 ml/kg body weight (for rats of 6 or more weeks old with oral administration), 5 ml/kg body weight (for rats of 5 or less weeks old with oral administration), or 10 ml/kg body weight (for mice with oral administration). Doses were designated in terms of milligram free-form TAK-418 per kilogram body weight.

Expression and purification of human LSD1-CoREST complex for enzyme assay

The experiment was performed as previously described (*35*). Expression plasmids, pET15SM/SUMO-hLSD1 (172 to 852) and pRH8/His-hCoREST (286 to 482), were cotransfected into competent *Escherichia coli* BL21 (DE3) cells. Transformed cells were grown in modified M9 medium supplemented with 1% yeast extract. Expression of proteins was induced by 1 mM isopropyl β-D-1-thiogalactopyranoside. Cells from a 3-liter culture were lysed by sonication, and His-SUMO-hLSD1 (172 to 852) and His-hCoREST (286 to 482) were purified using a nickel-nitrilotriacetic acid (Ni-NTA) superflow cartridge (30765, Qiagen) and HiLoad 26/60 Superdex 200 pg (28989336, GE Healthcare). His-SUMO tag at the N terminus of hLSD1 (172 to 852) was cleaved by SUMO protease (4010, LifeSensors). The SUMO protease and the cleaved His-SUMO tag were removed using reverse Ni-NTA chromatography. Human LSD1 (172 to 852) and His-hCoREST (286 to 482) complex were further purified with HiLoad 26/60 Superdex 200 pg equilibrated with phosphate-buffered saline (PBS) containing 150 mM NaCl and 5% (v/v) glycerol. Protein concentration was measured with a BCA protein assay kit (23225, Thermo Fisher Scientific) using bovine serum albumin (BSA) as the standard.

In vitro LSD1 enzyme kinetic assay for determination of k_{inact}/K_I values

Kinetics of in vitro LSD1 enzyme activity was measured with a peroxidase-coupled assay (*35*). Various concentrations of the compounds were incubated with 500 μM mono-methylated Lys 4 histone H3 peptide that was synthesized by Scrum Inc. in assay buffer [50 mM tris-HCl (pH 8.0) and 0.1% BSA]. After the addition of horseradish peroxidase (20 μg/ml; 31490, Thermo Fisher Scientific) and 50 μM AmplexRed reagent (A22177, Thermo Fisher Scientific), enzyme reaction was initiated by incubation with 20 nM recombinant LSD1/CoREST. The hydrogen peroxide production during amine oxidase reaction by LSD1 was monitored by AmplexRed reagent. The fluorescence signals of the resultant product resorufin were detected at 585 nm, with the excitation at 570 nm, by using Spectra Max (Molecular Devices). Because the compounds were irreversible inhibitors, their progress curve of fluorescent signals with background subtraction was fitted with Eq. 1, using GraphPad Prism 5 Software (GraphPad Software Inc.)

$$y = y_0 + (v_i/k_{obs})\left[1 - e(-k_{obs} * t)\right] \quad (1)$$

where v_i represents initial velocity, and k_{obs} and t demonstrate pseudo–first-order rate constant and time, respectively. y_0 is the product when t is 0. The estimated k_{obs} were replotted as a function of inhibitor concentration, and k_{inact} or K_I values were calculated from Eq. 2

$$k_{obs} = k_{inact}/\,[1 + (K_I/[I])\,(1 + [S]/K_m)\,] \quad (2)$$

where K_m value represents the concentration of histone H3 peptide substrate, evaluated at 20 μM.

In vitro LSD1 demethylase assay

Homogenous time-resolve fluorescence (HTRF) detection system (Cisbio Bioassays) was used to estimate in vitro LSD1 demethylation activity (*35*). Reaction buffer consisted of 50 mM tris-HCl (pH 8.0), 1 mM dithiothreitol (DTT), and 0.01% BSA. The demethylation reaction was started by adding 1 μM biotinylated mono-methylated Lys 4 histone H3 peptide [ART(mK)QTARKSTGGKAPRKQLAGGK-Biotin] (Scrum Inc.) to the enzyme (25 nM recombinant LSD1/CoREST) and then terminated by adding 1 mM *trans*-2-phenylcyclopropylamine after 40 min. The demethylated peptide was detected by cryptate-labeled anti–histone H3 antibody (64CUSKAZ, Cisbio Bioassays) and streptavidin-XLent! (611SAXLB, Cisbio Bioassays) diluted with detection buffer consisting of 800 mM KF and 0.1% BSA. After incubation at room temperature for 1 hour, the plates were read using EnVision 2102 Multilabel Reader (PerkinElmer). Total reaction was set as 0% inhibitory activity, and the reaction without enzyme was set as 100% inhibitory activity. Curve fittings and calculations of IC_{50} values with 95% confidence interval were performed with the program XLfit version 5 (ID Business Solutions Ltd.), with the maximum and minimum of the curve constrained to 100 and 0, respectively.

In vitro monoamine oxidase (MAO) A/B enzyme assay

MAOA/B enzyme activity was measured with MAO-Glo Assay (V1402, Promega) by following the manufacturer's instructions (*35*). MAOA and MAOB were purchased from Sigma-Aldrich. Briefly, a test compound was mixed with reaction solution containing MAOA or MAOB enzyme for 10 min, and then the reaction was started by adding MAO substrate. After the reaction at room temperature for 60 min, luciferin detection reagent was added to terminate the reaction. The luminescence was measured by EnVision. Luminescent signals of the complete reaction mixture were defined as 0% inhibitory activity, and those of the reaction without enzyme were defined as 100% inhibitory activity. Curve fittings and calculations of IC_{50} values were performed with the program XLfit version 5 with the maximum and minimum of the curve constrained to 100 and 0, respectively.

Primary neuronal culture

Cerebral cortex and hippocampus were isolated from fetal SD rats at embryonic day 19. Cell suspension was prepared using Nerve Cell Dissociation Medium (MS-0006L, Sumitomo Bakelite Co. Ltd.) and plated on a poly-L-lysine–coated plates at a density of 9.8×10^4 cells/cm^2. Under the conditions of 37°C and 5% CO_2, the cells were cultured in a Neurobasal medium (211103049, Invitrogen) containing B27 supplement (1:50 dilution; 17504044, Invitrogen), 2 mM L-glutamine (B76053, Lonza), penicillin (100 U/ml)/streptomycin (100 μg/ml) (17-602E, Lonza), and gentamicin sulfate (20 μg/ml; 17-519Z, Lonza).

TF-1a culture

TF-1a cells were purchased from American Tissue Culture Collection and were cultured under the conditions of 37°C and 5% CO_2 in RPMI 1640 (189-02145, Wako Pure Chemical Industries Ltd.) containing 10% fetal bovine serum (10099, Invitrogen). Cell viability was examined using CellTiter-Glo Luminescent Cell Viability Assay (G7570, Promega) according to the manufacturer's instructions.

ChIP-qPCR

Rat primary neuronal cultures after compound treatment for 1 or 3 days were harvested in ice-cold PBS by scraping. The cell pellets were collected by centrifugation at 3000 rpm for 5 min at 4°C and were subjected to ChIP procedures. Brain tissues from compound-treated mice were isolated and frozen-stored until ChIP procedures.

For ChIP–quantitative PCR (qPCR) analysis, ChIP was performed by using ChIP-IT Express Enzymatic (53009, Active Motif) and H3K4me2 antibody (07-030, Millipore) or H3K9me2 antibody (39239, Active Motif) with a slight modification according to the manufacturer's instruction; before chromatin digestion, nuclear pellets were washed with buffer containing 15 mM tris-HCl (pH 7.6), 15 mM NaCl, 60 mM KCl, 5 mM $MgCl_2$, 0.1 mM EGTA, 0.5 mM DTT, and 1.2 M sucrose. DNA fragments obtained by ChIP were used as a qPCR template. The qPCR was performed using the ABI PRISM 7900HT System (Applied Biosystems), SYBR Green Real-time PCR Master Mix -Plus- (QPK-212, TOYOBO), and the primers (rat *Ucp2*: forward primer 5′-TAGGAAGTCGCGAACCAGAG-3′ and reverse primer 5′-CTATTCCCCAGACGGACAGT-3′; rat *Bdnf*: forward primer 5′-AGGACAGCAAAGCCACAATG-3′ and reverse primer 5′-GAGCCGTGATATGCCTGTTG-3′).

Results are presented as % input, calculated as the percentage of ChIP DNA from the total amount of chromatin DNA (input DNA), according to the following formula

$$\%\ \text{input} = 2^{(\text{CtInput}-\text{CtChIP})} \times \text{Fd} \times 100(\%)$$

where CtInput and CtChIP represent the threshold cycle values of the input DNA and the ChIP sample, respectively, and Fd is the dilution factor of the input DNA.

Real-time qPCR

TAK-418 was dissolved in DMSO and diluted to give the final concentration of DMSO as 0.5% (v/v). To quantify mRNA expression levels in in vitro samples by reverse transcription (RT)–qPCR, the cells were harvested after 1 day (TF-1a cells) or 3 days (primary cultured rat neurons from days in vitro 10 to 13) of compound treatment, and a FastLane kit (216513, Qiagen) was used according to the manufacturer's instruction. RT-qPCR was carried out using an ABI PRISM 7900HT system (Life Technologies) or QuantStudio7 (Life Technologies). The expression level of *Ucp2* mRNA was normalized by those of *Ppia* mRNA. The expression level of *GFI1* mRNA was normalized by that of *GAPDH* mRNA (402869, Life Technologies). Primer and probe sequences used for real-time qPCR analysis are shown below.

Rat *Ucp2*: forward primer 5′-TTGCCCGAAATGCCATTGTC-3′, reverse primer 5′-GCAAGGGAGGTCGTCTGTC-3′, probe 5′-(FAM)-TGTACTGAGCTGGTGACCTATGACCTCATC-(TAMRA)-3′. Rat *Ppia*: forward primer 5′-GCTGATGGCGAGCCCTTG-3′, reverse primer 5′-CACGAAAGTTTTCTGCTGTCTTTG-3′, probe 5′-(FAM)-TGCAAACAGCTCGAAGCAGACGCGAC-(TAMRA)-3′. Human *GFI1*: forward primer 5′-TCACCCTCCGCGTCTCCA-3′, reverse primer 5′- CGCTCCATGAGTACGGTTTGA-3′, probe 5′-(FAM)-CTTCGTCCAGCGATGGGCACATTGACT-(TAMRA)-3′.

Immunoprecipitation

TF-1a cell pellets were lysed in lysis buffer containing 20 mM Hepes (pH 7.5), 25% glycerol, 0.2 mM EDTA, 150 mM KCl, 1.5 mM $MgCl_2$, 0.5% NP-40, and protease inhibitor cocktail (4693132, Roche) by

incubating for 15 min on ice, and pellets were obtained by centrifugation at 15,000 rpm at 4°C for 15 min. The pellets were treated with micrococcal nuclease (2 U/μl; 88216, Thermo Fisher Scientific) in buffer containing 20 mM Hepes (pH 7.5), 0.3 M sucrose, 200 mM KCl, 2 mM $MgCl_2$, 1 mM $CaCl_2$, 0.1% Triton X-100, and protease inhibitor cocktail (4693132, Roche) and incubated for 10 min at room temperature. The digestion reaction was stopped by adding 0.5 M EDTA. After centrifugation at 15,000 rpm for 10 min at 4°C, the supernatant was collected as a chromatin fraction. LSD1 protein contained in the chromatin fraction was immunoprecipitated by anti-LSD1 antibody (pAb-067-050, Diagenode) and Protein G Mag Sepharose (28-9513-79, GE Healthcare) according to the manufacturer's instructions, with a modification in wash steps; the beads were washed twice sequentially with buffers containing 100 and 300 mM KCl. LSD1 and GFI1B proteins bound to the sepharose beads were analyzed by Western blotting using NuPAGE LDS sample buffer (NP0007, Invitrogen), NuPAGE Protein Analysis System with NuPAGE Bis-Tris Gels (NP0323, Invitrogen), NuPAGE MOPS SDS Running Buffer (NP0001, Invitrogen), polyvinylidene difluoride membrane (LC20002, Invitrogen), NuPAGE transfer buffer (NP0006-1, Invitrogen), anti-LSD1 antibody (2139, Cell Signaling Technology), and anti-GFI1B antibody (sc-28356, Santa Cruz). The blots were developed using Immobilon Western Chemiluminescent HRP Substrate (WBKLS0100, Millipore).

Crystallization, data collection, and structure determination

Crystallization, data collection, and structure determination were performed as previously described (*12*) with minor modifications. Briefly, before crystallization experiments, the protein was incubated with 1 mM TAK-418 for 1 hour on ice. Crystals were obtained using the sitting-drop vapor diffusion method at 20°C by mixing a 70 nl of protein solution and a 70 nl of reservoir solution containing 0.1 M imidazole/HCl (pH 7.0), 14% PEG 3350, 10% 2-methyl-2,4-pentanediol, and 50 mM magnesium chloride for TAK-418. Before data collection, complex crystals were treated with a cryoprotectant solution composed of the reservoir solution with 2-methyl-2,4-pentanediol further added to 12.5% by volume of the total solution and were flash-frozen in liquid nitrogen. Diffraction data were collected from a single crystal at the Advanced Light Source beamline 5.0.2 (Berkeley, CA) at 100 K and processed using the program HKL2000. The structures were determined by molecular replacement using MOLREP, using the previously reported coordinate of LSD1 with the PDB accession code 2Z5U. Subsequently, the structures were refined through an iterative procedure using REFMAC followed by model building with WinCoot (version 0.3.3). The dictionary files for the FAD-compound adducts were prepared using AFITT CL (OpenEye Scientific Software).

Analysis of FAD adducts with TAK-418 in LSD1 protein by ESI-TOF mass spectrometry

Human recombinant LSD1 protein (125 μM) was treated with 1 mM TAK-418 at room temperature for 1 hour in 50 mM tris-HCl (pH 8.0) to form TAK-418 adducts on FAD in LSD1. Subsequently, the protein samples were denatured on ice with adding 8 M urea solution to a final concentration of 6.4 M for 1 hour, and the FAD-compound adducts were extracted on ice with acetonitrile for 15 min. The precipitates were removed by centrifugation. The supernatants were added 500 mM ammonium acetate to a final concentration of 5 mM and were subjected to electrospray ionization (ESI) mass spectrometric analysis. The samples containing FAD-compound adducts were analyzed by Waters LCT premier, single time-of-flight (TOF) liquid chromatography–mass spectrometry (LC-MS) system, using the negative ion detection mode. Unizon UK-18 (Imtakt) was used for LC separation column, and 10 mM ammonium acetate was used for LC solvent. The eluate was carried out with 0 to 100% acetonitrile. Column and solvent were chilled with ice for suppressing degradation of the FAD-compound adducts during all the procedure.

Ex vivo LSD1 enzyme assay

Cortical or hippocampal tissues were isolated from the mice administered with compounds and were frozen-stored until the assay. The control tissues were isolated from the rats at 2 hours after vehicle treatment. Tissues were homogenized in radioimmunoprecipitation assay buffer (20-188, Millipore) containing protease inhibitor cocktail (4693132001, Roche) and phosphatase inhibitor cocktail (4906837001, Roche) and were precleared by Protein G Sepharose 4FF (17-0618-01, GE Healthcare). Then, LSD1 protein in the homogenate was immunoprecipitated by using anti-LSD1 antibody (2139, Cell Signaling Technology) and Protein G Sepharose 4FF, according to the manufacturer's instructions. Histone demethylase activity in the immunoprecipitates was measured by HTRF detection system, using biotin-labeled monomethyl-H3K4 peptide (Scrum Inc.), europium cryptate-labeled anti–histone H3 antibody (64CUSKAZ, Cisbio Bioassays), and Streptavidin-XLent! (611SAXLB, Cisbio Bioassays), and the remaining demethylase activity was determined by HTRF ratio (time-resolved fluorescence at 665 nm/time-resolved fluorescence at 615 nm).

Blood toxicity studies

Blood samples were collected in vacuum blood collection tubes containing EDTA-2K (for rats) or in collection tubes containing EDTA-2K (for mice). White blood cells, red blood cells, and platelets in the whole blood samples were counted using an automated hematology analyzer (ADVIA2120i, Siemens Healthcare Diagnostics K.K. or XT-1800i, Sysmex Corporation) and standard reagents (CBC TIMEPAC, T01-3620-52 or e-Check, XFN-110A, Sysmex Corporation).

Determination of TAK-418 plasma concentrations

Analyses were performed by Nishiwaki Laboratory, CMIC Pharma Science Co. Ltd., or Axcelead Drug Discovery Partners Inc. Whole blood was collected from the TAK-418–treated rats or mice, and plasma was isolated by centrifugation at 17,400*g* for 1 min or at 13,000*g* for 15 min at 4°C. Plasma concentrations of TAK-418 were measured by LC–tandem MS systems.

Generation of VPA rats

Study design

The sample sizes in the behavioral experiments using VPA rats are shown in each figure legend. In Fig. 5G, each litter was considered an experimental unit. For other data, each animal was considered an experimental unit. The RNA-seq experiments were performed with three replicated samples. Each sample was generated from pooled independent cortical tissues taken from three different rats. ChIP-seq and RRBS experiments were performed with three replicated samples, each sample was generated from pooled independent cortical tissues taken from 9 or 10 different rats. The numbers of pups and dams used in each experiment are shown in table S4. The rats were

allocated to each group (VPA-vehicle or VPA-TAK-418) to balance their body weights between groups.

Experimental procedures

Sodium salt VPA (Sigma, P4543, lot MKBS5273V) was dissolved in 0.9% NaCl (saline) and intraperitoneally injected into the pregnant SD rats at 500 mg/(2 ml/kg) on GD12.5, without change of cage. The VPA solution was prepared immediately before use and adjusted to a neutral pH with hydrochloric acid. The light cycle of the animal housing room was 7:00 on/19:00 off. The time of day of injection was 13:00 to 17:00. The room temperature at injection time was 23°C (20° to 26°C). The gestational timing was validated by vaginal plug observation.

Experimental animals

Pregnant SD rats were purchased from Charles River Laboratories, Japan. The maternal age at challenge was 9 to 12 weeks, and the maternal body weight was 256 to 385 g. Only male offspring were tested in this study, with body weights of 45.5 to 65.2 g (control rats) and 31.0 to 61.9 g (VPA rats) at weaning (3 weeks old). The animal ages at the time of testing are shown in each figure legend.

Housing and husbandry

Breeding was performed at Charles River Laboratories, Japan. The light cycle of the animal housing room was 6:00 on/18:00 off, and room temperature was 20° to 25°C. The type of cage bedding used was Howaitofure-ku or Sanfure-ku (Oriental Yeast Co. Ltd.). The success rate of pregnancy for dams was 98.9% (recorded in 2019). After plug check, the dams were handled only during cage changes. The sires were 30 to 40 weeks old. The numbers of sires and dams that were bred were the same. The success rate of pregnancy for sires was 91.0% (recorded in 2019). The sires from unsuccessful matings were removed from breeding. The interval between mating times was at least 2 days. Sires were not matched specifically to experimental or control dams. A 1:1 mating design was used.

The pregnant rats were shipped to Takeda Pharmaceutical Company Limited on GD6. The light cycle of the animal housing room was 7:00 on/19:00 off, and room temperature was 23°C (20° to 26°C). Humidity in the room was 55% (40 to 70%). The ventilation system was heating ventilation and air conditioning (HVAC), one-way airflow rack, and specific pathogen free (SPF). The type of cage bedding used was Care-feeaz (HAMRI Co. Ltd.) and Paper-clean (Japan SLC Inc.). The cages were changed three times during gestation, once at postnatal day 7, and twice per week after weaning. The litters were weaned and sexed on postnatal day 21 and divided into several cages (two to three rats per cage).

The material of cage is plastic. Before breeding, not more than 16 female or 6 male rats were housed per cage (345 mm by 540 mm by 200 mm) or a maximum of 3 male rats were housed per cage (292 mm by 440 mm by 200 mm). The dams were separated for parturition on GD6 with one Nylon Bone (Bio-Serv) per cage (500 mm by 355 mm by 198 mm). After weaning, there were two or three rats per cage (247 mm by 355 mm by 198 mm or 500 mm by 355 mm by 198 mm) with one I Chew (ASAP) per cage as physical enrichment.

Experimental design

The cognition test in 6-week-old rats (Fig. 6A) was carried out 2, 3, or 6 days after the sociability test. In other experiments, only one behavior test per rat was performed. For data analysis, the number of animals represented the unit of each analysis. The rats that did not sniff stranger rats, or objects in the sociability test were removed from the analysis. The methods of statistical analysis are given in each figure legend.

Generation of poly I:C mice

Study design

The sample sizes in the behavioral experiments using poly I:C mice are shown in each figure legend. Each animal was considered an experimental unit. The RNA-seq experiments were performed with three replicated samples. Each sample was generated from pooled independent cortical tissues taken from six different mice. ChIP-seq and RRBS experiments were performed with three replicated samples, each sample was generated from pooled independent cortical tissues taken from five or six different mice. The numbers of pups and dams used in each experiment are shown in table S4. The mice were allocated to each group (poly I:C-vehicle or poly I:C–TAK-418) to balance their body weights between groups by using statistical software, EXSUS (CAC Croit Corporation).

Experimental procedures

Poly I:C potassium salt (P9582, lot 075M4076V, Sigma-Aldrich) was dissolved in 0.9% (w/v) NaCl to achieve a concentration of 1 mg/ml and was administered to pregnant C57BL/6J mice on GD15 at 5 mg/(5 ml/kg) via tail vein, without change of cage or anesthetic. The poly I:C solution was prepared immediately before use. The light cycle of the animal housing room was 7:00 on/19:00 off. The time of day of injection was 13:00 to 16:00. The room temperature at injection time was 23°C (20° to 26°C). Maternal cytokine levels 1 to 2 hours after an intravenous injection of poly I:C (5 mg/kg; Sigma-Aldrich, P9582, lot 075M4076V) on GD15 were analyzed by the V-PLEX Proinflammatory Panel 1 Mouse Kit (MSD, K15048D). There was a potent up-regulation of interleukin-6 (IL-6), IL-10, keratinocyte-derived chemokine/growth-related oncogene, and tumor necrosis factor–α levels in the plasma, suggesting a potent immune response (fig. S3). The gestational timing was validated by vaginal plug observation.

Experimental animals

Pregnant C57BL/6J mice were purchased from CLEA Japan Inc. The maternal age at challenge was 14 to 16 weeks, and the maternal body weight was 26 to 38 g. Only male offspring were tested in this study, with a body weight of 26 to 37 g at sociability test (22 weeks old).

Housing and husbandry

Breeding was performed at CLEA Japan Inc. The type of cage bedding used was wood chip. Primiparous and multiparous dams were used. The success rate of pregnancy for dams was 80%. After plug check, the dams were handled only during cage changes and weighing. The sires were 12 weeks old or older. Sires were used until success rate fell but were not used more than a year. The sires that failed matings twice in a row were removed from breeding. The interval between mating times was at least 2 days. Sires were not matched specifically to experimental or control dams. A 1:1 mating design was used. The numbers of sires and dams that were bred were not disclosed from the vendor.

The pregnant mice were shipped to Takeda Pharmaceutical Company Limited on GD6. The light cycle of the animal housing room was 7:00 on/19:00 off, and room temperature was 23°C (20° to 26°C). Humidity in the room was 55% (40 to 70%). The ventilation system was HVAC, one-way airflow rack, SPF. The type of cage bedding used was ALPHA-dri (Shepherd Specialty Papers Inc.). The cages were changed once before poly I:C injection on GD15 and once per week after postnatal day 8. The litters were weaned and sexed on postnatal day 21 and divided into several cages (three to four mice per cage).

The material of cage is plastic. Before breeding, 10 to 13 mice were housed per cage (182 mm by 260 mm by 128 mm). The dams were separated for parturition on GD6 with one I Chew (ASAP) and one shelter made of wood pulp per cage (185 mm by 332 mm by 147 mm) as

physical enrichment. After weaning, there were three or four mice per cage (185 mm by 332 mm by 147 mm) with one I Chew per cage as physical enrichment. I Chew was changed to new one at cage changes and across studies.

Experimental design

Litter size was 3 to 10, and one to six males and one to six females in each litter were maintained. Female pups were culled at weaning, and male pups were culled after sociability test. Each dam raised her own litters. Only one behavior test per mouse was performed at 22 weeks of age. Maternal care was not evaluated. For data analysis, the number of animals represented the unit of each analysis. The methods of statistical analysis are given in each figure legend.

RNA sequencing

Cortical tissues for RNA-seq analysis were isolated from VPA rats or poly I:C mice and from respective control animals and stored frozen until use. Total RNA was extracted using the RNeasy Mini QIAcube Kit (74116, Qiagen). RNA-seq experiments were performed by Takara Bio Inc. using a HiSeq 2000 sequencer (Illumina), which generated 40 million 100–base-paired end reads for each sample. The sequence reads were mapped to rat genomes (rn6) or mouse genomes (mm10). Hierarchical clustering was performed on the basis of the cosine similarity and complete linkage method for $\log_2$-transformed count per million data. The clustering results were visualized using the ComplexHeatmap package in R software (*36*). The samples were divided into two clusters by a static tree cut. Scatter plots were created using R software. DEGs with FDRs < 0.2 were identified by Voom after trimmed mean of M-value normalization. Correlation coefficients were calculated using Pearson's correlation analysis. Linear regression was performed to fit the data points on the scatter plot. The biological pathways from Molecular Signature Database (CP: Canonical pathways including REACTOME, BIOCARTA, Pathway Interaction Database, and Kyoto Encyclopedia of Genes and Genomes) enriched in the DEGs were analyzed by GSEA.

Chromatin immunoprecipitation sequencing

ChIP-seq experiments were performed using cortical tissues from VPA rats at 5 weeks of age and poly I:C mice at 22 weeks of age, after 2 weeks of vehicle or TAK-418 administration at 1 mg/kg, and from respective control animals. The cortical tissues were isolated and stored frozen until use. ChIP-seq assays using antibodies against H3K4me3 (39159, Active Motif), H3K9me3 (39161, Active Motif), H3K9ac (39159, Active Motif), or H3K27me3 (39155, Active Motif) were performed by Active Motif Inc. using their proprietary methods. The sequence reads were mapped to rat genomes (rn5) or mouse genomes (mm10). The peaks were called using the spatial clustering for identification of ChIP-enriched regions (SICER) algorithm. The overlapping peaks between samples were grouped into MergedRegions. Spike-in adjusted normalization was performed. Peaks located ±7500 bp relative to TSSs were used for the calculation of FC of read density for each MergedRegion. Differentially modified genomic regions (FDR < 0.2) were identified by *t* test based on read density. Scatter plots were generated using R software, and correlation coefficient values were calculated using Pearson's correlation analysis. Linear regression was performed to fit the data points on the scatter plot.

DNA methylation analysis

RRBS was performed using cortical tissues from VPA rats at 5 weeks of age and poly I:C mice at 22 weeks of age, after 2 weeks of vehicle or TAK-418 administration at 1 mg/kg and from control animals. Cortical tissues for RRBS were isolated from hemi-brains of the animals used for ChIP-seq studies and stored frozen until use. RRBS was performed by Active Motif using their proprietary methods. The sequence reads were mapped to rat genomes (rn6) or mouse genomes (mm10). The proportions of DNA methylation within 0 to 2000 bp upstream of the TSSs were calculated. Coverage must exceed the minimum (three CpGs with three reads per CpG) for all samples to be included. Differentially modified genomic regions (FDR < 0.2) were identified by *t* test based on the difference of methylation ratio. Scatter plots were generated using R software, and correlation coefficient values were calculated using Pearson's correlation analysis. Linear regression was performed to fit the data points on the scatter plot.

Sociability test in VPA rats

Sociability test using VPA rats was performed by Takeda Pharmaceutical Company Limited or Axcelead Drug Discovery Partners Inc. A three-chambered sociability test was performed at 5, 6, and 15 weeks of age in control and VPA rats. TAK-418 at 1 mg/kg or vehicle was orally administered 2 hours before testing (single administration). Alternatively, TAK-418 at 0.1, 0.3, or 1 mg/kg or vehicle were orally administered once daily (QD) for 14 days, starting from 3 to 5 weeks of age or from 13 to 15 weeks of age (repeated administration). The apparatus was a three-chamber box (each chamber: 30 cm by 60 cm by 34 cm), with dividing walls made from transparent plates and containing a gate (10 cm by 12 cm). In the two outer chambers, transparent cylinders with small holes (cylinder: 12 cm ϕ × 25 cm; hole: 1.5 cm ϕ for 5-week-old rats and 2 cm ϕ for 15-week-old rats) were placed to avoid direct physical interactions between rats. The sociability test involved a stranger rat and an inanimate object (white sphere). A rat of the same strain and the same age as the test rats was used as the stranger. On the day of testing, all rats were separately allowed to acclimate to the test room for more than 1 hour before testing. A control or VPA rat was then introduced into the middle chamber for 5 min with the gate closed. A stranger was then introduced into one of the cylinders. An inanimate object (white sphere) was placed in the other cylinder. Then, by gently removing the gates, the test animal was allowed to explore all three chambers freely. The time spent sniffing each cylinder was scored manually for 10 min. The sniffing index was calculated using the following equation

$$\text{Sniffing index} = [\text{sniffing time to stranger cylinder (s)} - \text{sniffing time to inanimate cylinder (s)}]/\text{total sniffing time(s)}]$$

Sociability test in poly I:C mice

A three-chambered sociability test was performed at 22 weeks of age in control and poly I:C mice. TAK-418 at 0.1, 0.3, or 1 mg/kg or vehicle were administered QD for 14 days starting from 20 to 22 weeks of age. The apparatus was a three-chamber box (center chamber: 14.5 cm by 19 cm by 21.5 cm; outer chambers: 19.3 cm by 19 cm by 21.5 cm), with dividing walls made from transparent plate and containing a gate (8 cm by 8 cm). In the two outer chambers, transparent cylinders with small holes (8.2 cm ϕ × 20.5 cm; hole: 1.3 cm ϕ) were placed to avoid direct physical interactions between mice. The sociability test involved a stranger mouse. A mouse of the same strain and the same age as the test mice was used as the stranger. Mice were habituated to the test arena without cylinders for 5 min with cage

mates, 2 days before test, and they were individually habituated to the test arena without cylinders for 5 min, 1 day before the test. On the day of testing, all mice were separately allowed to acclimate to the test room for more than 1 hour before testing. A control or poly I:C mouse was introduced in the middle chamber for 3 min with the gate closed. A stranger was then introduced into one of the cylinders. Then, by gently removing the gates, the test animal was allowed to explore all three chambers freely. The time spent sniffing each cylinder was scored manually for 5 min. The sniffing index was calculated using the following equation:

$$\text{Sniffing index} = [\text{sniffing time to stranger cylinder (s)} - \text{sniffing time to inanimate cylinder (s)}]/\text{total sniffing time(s)}]$$

NOR test

NOR tests for cognitive deficit were performed using 6-week-old control and VPA rats (*37*) following the sociability test. TAK-418 (0.1 and 1 mg/kg) or vehicle was orally administered QD for about 16 to 20 days starting from 3 weeks of age to the day before testing. On the day before testing, rats were allowed to acclimate to the test room for more than 1 hour, and they were then allowed to habituate to the empty test box (a gray-colored polyvinyl chloride box of 40 cm by 40 cm by 50 cm) for 10 min individually. Testing comprised two 3-min trials for acquisition and retention that were separated by a 4-hour intertrial interval (ITI). On the day following the final administration, control or VPA rats were allowed to explore two identical objects (A1 and A2) for 3 min (the acquisition trial). Then, 4 hours after the acquisition trial, they were again allowed to explore a familiar object (A3) and a novel object (B) for 3 min.

NOR tests were performed, using naïve 7-week-old male Long-Evans rats, to assess delay-dependent forgetting. Tests were performed as described above, with minor modifications. Rats were allowed to habituate to the behavioral test room environment for more than 1 hour on day 1 and were then allowed to habituate to the empty test box, described above, for 10 min individually. Testing comprised two 3-min trials for acquisition and retention that were separated by a 48-hour ITI. On day 2, rats were allowed to explore two identical objects (A1 and A2) for 3 min in the acquisition trial. On day 4, rats were again allowed to explore a familiar object (A3) and a novel object (B) for 3 min in the retention trial. TAK-418 (0.1 and 1 mg/kg) or vehicle was administered once (single administration) or QD for 2 weeks (14 days, repeated administration). The single administration and the final administration of repeated administrations were performed 2 hours before the acquisition trial.

Object exploration was defined as licking, sniffing, or touching the object with forelimbs while sniffing. Leaning against the object to look upward and standing or sitting on the object were excluded. Exploration times were scored manually for each object (A1, A2, A3, and B) in each trial. The NDI was calculated as the exploration time for the novel object/total exploration time.

Open field test for evaluation of repetitive behavior

Repetitive behaviors were evaluated by open field test at 5 weeks of age in control and VPA rats. TAK-418 at 1 mg/kg or vehicle was orally administered once daily for 14 days, starting from 3 to 5 weeks of age. The apparatus was a black plastic box (50 cm by 50 cm by 35 cm). On the day of testing, all rats were allowed to acclimate to the test room for more than 1 hour, and a control or VPA rat was introduced into the box and allowed to explore freely. The time spent self-grooming (scratching and brushing the hair with its forelimbs or mouth) in the open field during a 20-min period was measured manually through video recording.

Y-maze test for evaluation of repetitive behavior

Repetitive behaviors were evaluated by spontaneous alternation activities represented by alternation ratio and alteration scores in Y-maze test. The apparatus was a Y-maze (arm length: 46 cm; arm width: 8 cm; height of wall: 30 cm) constructed of clear plastic covered with black paper. On the day of testing, 5-week-old control and VPA rats were allowed to acclimate to the test room for more than 1 hour. For the evaluation by alternation ratio, each rat was placed at the end of one arm and allowed to freely explore the maze for 8 min. The sequence of arm entries was counted manually through video recording. The percentage of alternation (alternation ratio) was calculated as the ratio of actual to maximum number of alternations. For the evaluation by alternation scores, each rat was placed at the end of the start arm and allowed to freely choose a goal arm from the other two arms. The session was repeated five times, and the subsequent arm choice was counted manually. The alternation score was defined as the number of alternations of subsequent goal arm entry.

Statistical analysis

Data were presented as means + SEM (in the results of behavioral studies) or SD (other studies). *F* tests followed by Student's *t* tests (for data with homoscedasticity) or Aspin-Welch tests (for data with heteroscedasticity) were used to assess the significance of the differences between groups. Bartlett's tests, followed by one-tailed Williams tests (for data with homoscedasticity) or one-tailed Shirley-Williams tests (for data with heteroscedasticity) were used to assess the significance of the concentration- or dose-dependent differences, compared to control groups. The parametric Dunnett's test was used to assess the significance of the time-dependent differences compared to control groups. For in vitro data with $N = 3$ per group, a parametric test was selected, without an *F* test or Bartlett's test. Bonferroni correction was used to adjust for multiple comparisons. The criteria for significance are indicated in each figure legend.

SUPPLEMENTARY MATERIALS

Supplementary material for this article is available at http://advances.sciencemag.org/cgi/content/full/7/11/eaba1187/DC1

View/request a protocol for this paper from *Bio-protocol*.

REFERENCES AND NOTES

1. S. De Rubeis, X. He, A. P. Goldberg, C. S. Poultney, K. Samocha, A. E. Cicek, Y. Kou, L. Liu, M. Fromer, S. Walker, T. Singh, L. Klei, J. Kosmicki, F. Shih-Chen, B. Aleksic, M. Biscaldi, P. F. Bolton, J. M. Brownfeld, J. Cai, N. G. Campbell, A. Carracedo, M. H. Chahrour, A. G. Chiocchetti, H. Coon, E. L. Crawford, S. R. Curran, G. Dawson, E. Duketis, B. A. Fernandez, L. Gallagher, E. Geller, S. J. Guter, R. S. Hill, J. Ionita-Laza, P. J. Gonzalez, H. Kilpinen, S. M. Klauck, A. Kolevzon, I. Lee, I. Lei, J. Lei, T. Lehtimaki, C. F. Lin, A. Ma'ayan, C. R. Marshall, A. L. McInnes, B. Neale, M. J. Owen, N. Ozaki, M. Parellada, J. R. Parr, S. Purcell, K. Puura, D. Rajagopalan, K. Rehnstrom, A. Reichenberg, A. Sabo, M. Sachse, S. J. Sanders, C. Schafer, M. Schulte-Ruther, D. Skuse, C. Stevens, P. Szatmari, K. Tammimies, O. Valladares, A. Voran, W. Li-San, L. A. Weiss, A. J. Willsey, T. W. Yu, R. K. Yuen; DDD Study; Homozygosity Mapping Collaborative for Autism; UK10K Consortium, E. H. Cook, C. M. Freitag, M. Gill, C. M. Hultman, T. Lehner, A. Palotie, G. D. Schellenberg, P. Sklar, M. W. State, J. S. Sutcliffe, C. A. Walsh, S. W. Scherer, M. E. Zwick, J. C. Barett, D. J. Cutler, K. Roeder, B. Devlin, M. J. Daly, J. D. Buxbaum, Synaptic, transcriptional and chromatin genes disrupted in autism. *Nature* **515**, 209–215 (2014).
2. A. D. Rasalam, H. Hailey, J. H. Williams, S. J. Moore, P. D. Turnpenny, D. J. Lloyd, J. C. Dean, Characteristics of fetal anticonvulsant syndrome associated autistic disorder. *Dev. Med. Child Neurol.* **47**, 551–555 (2005).

3. I. Knuesel, L. Chicha, M. Britschgi, S. A. Schobel, M. Bodmer, J. A. Hellings, S. Toovey, E. P. Prinssen, Maternal immune activation and abnormal brain development across CNS disorders. *Nat. Rev. Neurol.* **10**, 643–660 (2014).
4. S. Nardone, E. Elliott, The interaction between the immune system and epigenetics in the etiology of Autism spectrum disorders. *Front. Neurosci.* **10**, 329 (2016).
5. C. Madore, Q. Leyrolle, C. Lacabanne, A. Benmamar-Badel, C. Joffre, A. Nadjar, S. Layé, Neuroinflammation in Autism: Plausible role of maternal inflammation, dietary omega 3, and microbiota. *Neural Plast.* **2016**, 3597209 (2016).
6. C. C. Wong, E. L. Meaburn, A. Ronald, T. S. Price, A. R. Jeffries, L. C. Schalkwyk, R. Plomin, J. Mill, Methylomic analysis of monozygotic twins discordant for autism spectrum disorder and related behavioural traits. *Mol. Psychiatry* **19**, 495–503 (2014).
7. D. Posthuma, T. J. Polderman, What have we learned from recent twin studies about the etiology of neurodevelopmental disorders? *Curr. Opin. Neurol.* **26**, 111–121 (2013).
8. C. Wynder, L. Stalker, M. L. Doughty, Role of H3K4 demethylases in complex neurodevelopmental diseases. *Epigenomics* **2**, 407–418 (2010).
9. C. N. Vallianatos, S. Iwase, Disrupted intricacy of histone H3K4 methylation in neurodevelopmental disorders. *Epigenomics* **7**, 503–519 (2015).
10. Y. Shi, F. Lan, C. Matson, P. Mulligan, J. R. Whetstine, P. A. Cole, R. A. Casero, Y. Shi, Histone demethylation mediated by the nuclear amine oxidase homolog LSD1. *Cell* **119**, 941–953 (2004).
11. Y. C. Zheng, J. Ma, Z. Wang, J. Li, B. Jiang, W. Zhou, X. Shi, X. Wang, W. Zhao, H. M. Liu, A systematic review of histone lysine-specific demethylase 1 and its inhibitors. *Med. Res. Rev.* **35**, 1032–1071 (2015).
12. H. P. Mohammad, K. N. Smitheman, C. D. Kamat, D. Soong, K. E. Federowicz, G. S. Van Aller, J. L. Schneck, J. D. Carson, Y. Liu, M. Butticello, W. G. Bonnette, S. A. Gorman, Y. Degenhardt, Y. Bai, M. T. McCabe, M. B. Pappalardi, J. Kasparec, X. Tian, K. C. McNulty, M. Rouse, P. McDevitt, T. Ho, M. Crouthamel, T. K. Hart, N. O. Concha, C. F. McHugh, W. H. Miller, D. Dhanak, P. J. Tummino, C. L. Carpenter, N. W. Johnson, C. L. Hann, R. G. Kruger, A DNA hypomethylation signature predicts antitumor activity of LSD1 inhibitors in SCLC. *Cancer Cell* **28**, 57–69 (2015).
13. S. Matsuda, R. Baba, H. Oki, S. Morimoto, M. Toyofuku, S. Igaki, Y. Kamada, S. Iwasaki, K. Matsumiya, R. Hibino, H. Kamada, T. Hirakawa, M. Iwatani, K. Tsuchida, R. Hara, M. Ito, H. Kimura, T-448, a specific inhibitor of LSD1 enzyme activity, improves learning function without causing thrombocytopenia in mice. *Neuropsychopharmacology* **44**, 1505–1512 (2019).
14. F. I. Roullet, J. K. Lai, J. A. Foster, *In utero* exposure to valproic acid and autism—A current review of clinical and animal studies. *Neurotoxicol. Teratol.* **36**, 47–56 (2013).
15. C. Nicolini, M. Fahnestock, The valproic acid-induced rodent model of autism. *Exp. Neurol.* **299**, 217–227 (2018).
16. U. Meyer, Prenatal poly(i:C) exposure and other developmental immune activation models in rodent systems. *Biol. Psychiatry* **75**, 307–315 (2014).
17. F. S. Mueller, J. Richetto, L. N. Hayes, A. Zambon, D. D. Pollak, A. Sawa, U. Meyer, U. Weber-Stadlbauer, Influence of poly(I:C) variability on thermoregulation, immune responses and pregnancy outcomes in mouse models of maternal immune activation. *Brain Behav. Immun.* **80**, 406–418 (2019).
18. J. Richetto, R. Massart, U. Weber-Stadlbauer, M. Szyf, M. A. Riva, U. Meyer, Genome-wide DNA methylation changes in a mouse model of infection-mediated neurodevelopmental disorders. *Biol. Psychiatry* **81**, 265–276 (2017).
19. J. Wang, S. Hevi, J. K. Kurash, H. Lei, F. Gay, J. Bajko, H. Su, W. Sun, H. Chang, G. Xu, F. Gaudet, E. Li, T. Chen, The lysine demethylase LSD1 (KDM1) is required for maintenance of global DNA methylation. *Nat. Genet.* **41**, 125–129 (2009).
20. C.-L. Lin, Y.-C. Hsu, Y.-T. Huang, Y.-H. Shih, C.-J. Wang, W.-C. Chiang, P.-J. Chang, A KDM6A-KLF10 reinforcing feedback mechanism aggravates diabetic podocyte dysfunction. *EMBO Mol. Med.* **11**, e9828 (2019).
21. E. Toska, P. Castel, S. Chhangawala, A. Arruabarrena-Aristorena, C. Chan, V. C. Hristidis, E. Cocco, M. Sallaku, G. Xu, J. Park, G. Minuesa, S. G. Shifman, N. D. Socci, R. Koche, C. S. Leslie, M. Scaltriti, J. Baselga, PI3K inhibition activates SGK1 via a feedback loop to promote chromatin-based regulation of ER-dependent gene expression. *Cell Rep.* **27**, 294–306.e5 (2019).
22. K. E. Hargis, E. M. Blalock, Transcriptional signatures of brain aging and Alzheimer's disease: What are our rodent models telling us? *Behav. Brain Res.* **322**, 311–328 (2017).
23. C. L. Brinkmeyer-Langford, J. Guan, G. Ji, J. J. Cai, Aging shapes the population-mean and -dispersion of gene expression in human brains. *Front. Aging Neurosci.* **8**, 183 (2016).
24. U. Meyer, J. Feldon, M. Schedlowski, B. K. Yee, Towards an immuno-precipitated neurodevelopmental animal model of schizophrenia. *Neurosci. Biobehav. Rev.* **29**, 913–947 (2005).
25. J. Richetto, U. Meyer, Epigenetic modifications in Schizophrenia and related disorders: Molecular scars of environmental exposures and source of phenotypic variability. *Biol. Psychiatry* **89**, 215–226 (2021).
26. M. Varghese, N. Keshav, S. Jacot-Descombes, T. Warda, B. Wicinski, D. L. Dickstein, H. Harony-Nicolas, S. De Rubeis, E. Drapeau, J. D. Buxbaum, P. R. Hof, Autism spectrum disorder: Neuropathology and animal models. *Acta Neuropathol.* **134**, 537–566 (2017).
27. E. P. Zorrilla, Multiparous species present problems (and possibilities) to developmentalists. *Dev. Psychobiol.* **30**, 141–150 (1997).
28. S. E. Lazic, L. Essioux, Improving basic and translational science by accounting for litter-to-litter variation in animal models. *BMC Neurosci.* **14**, 37 (2013).
29. S. E. Lazic, The problem of pseudoreplication in neuroscientific studies: Is it affecting your analysis? *BMC Neurosci.* **11**, 5 (2010).
30. A. C. Kentner, S. D. Bilbo, A. S. Brown, E. Y. Hsiao, A. K. McAllister, U. Meyer, B. D. Pearce, M. V. Pletnikov, R. H. Yolken, M. D. Bauman, Maternal immune activation: Reporting guidelines to improve the rigor, reproducibility, and transparency of the model. *Neuropsychopharmacology* **44**, 245–258 (2019).
31. Y. Katayama, M. Nishiyama, H. Shoji, Y. Ohkawa, A. Kawamura, T. Sato, M. Suyama, T. Takumi, T. Miyakawa, K. I. Nakayama, CHD8 haploinsufficiency results in autistic-like phenotypes in mice. *Nature* **537**, 675–679 (2016).
32. J. B. Tagne, O. R. Mohtar, J. D. Campbell, M. Lakshminarayanan, J. Huang, A. C. Hinds, J. Lu, M. I. Ramirez, Transcription factor and microRNA interactions in lung cells: An inhibitory link between NK2 homeobox 1, miR-200c and the developmental and oncogenic factors Nfib and Myb. *Respir. Res.* **16**, 22 (2015).
33. A. Sprussel, J. H. Schulte, S. Weber, M. Necke, K. Handschke, T. Thor, K. W. Pajtler, A. Schramm, K. Konig, L. Diehl, P. Mestdagh, J. Vandesompele, F. Speleman, H. Jastrow, L. C. Heukamp, R. Schule, U. Duhrsen, R. Buettner, A. Eggert, J. R. Gothert, Lysine-specific demethylase 1 restricts hematopoietic progenitor proliferation and is essential for terminal differentiation. *Leukemia* **26**, 2039–2051 (2012).
34. J. S. Huang, T. A. Lee, M. C. Lu, Prenatal programming of childhood overweight and obesity. *Matern. Child Health J.* **11**, 461–473 (2007).
35. Y. Ishikawa, K. Gamo, M. Yabuki, S. Takagi, K. Toyoshima, K. Nakayama, A. Nakayama, M. Morimoto, H. Miyashita, R. Dairiki, Y. Hikichi, N. Tomita, D. Tomita, S. Imamura, M. Iwatani, Y. Kamada, S. Matsumoto, R. Hara, T. Nomura, K. Tsuchida, K. Nakamura, A novel LSD1 inhibitor T-3775440 disrupts GFI1B-containing complex leading to transdifferentiation and impaired growth of AML cells. *Mol. Cancer Ther.* **16**, 273–284 (2017).
36. Z. Gu, R. Eils, M. Schlesner, Complex heatmaps reveal patterns and correlations in multidimensional genomic data. *Bioinformatics* **32**, 2847–2849 (2016).
37. E. Shiraishi, K. Suzuki, A. Harada, N. Suzuki, H. Kimura, The phosphodiesterase 10A selective inhibitor TAK-063 improves cognitive functions associated with Schizophrenia in rodent models. *J. Pharmacol. Exp. Ther.* **356**, 587–595 (2016).
38. Y. Hattori, K. Aoyama, J. Maeda, N. Arimura, Y. Takahashi, M. Sasaki, M. Fujinaga, C. Seki, Y. Nagai, K. Kawamura, T. Yamasaki, M. R. Zhang, M. Higuchi, T. Koike, Design, synthesis, and evaluation of (4R)-1-{3-[2-(^{18}F)Fluoro-4-methylpyridin-3-yl]phenyl}-4-[4-(1,3-thiazol-2-ylcarbonyl) piperazin-1-yl]pyrrolidin-2-one ([^{18}F]T-401) as a novel positron-emission tomography imaging agent for monoacylglycerol lipase. *J. Med. Chem.* **62**, 2362–2375 (2019).

Acknowledgments: We thank H. Kamada, T. Hirakawa, T. Niimura, M. Terada, M. Suzuki, T. Inoue, T. Takeuchi, M. Nomura, and M. Iwatani for pharmacological analysis; S. Okubo and Y. Awasaki for blood toxicity study; S. Iwasaki, K. Matsumiya, and A. Kogame for PK analysis; K. Yamamoto, K. Kimoto, and J. Takeda for physicochemical characterization of TAK-418; Y. Zama for preparing recombinant proteins; G. Snell and W. Lane for collecting and processing diffraction data; and E. Ratti for continuous support and encouragement for the TAK-418 program. **Funding:** This work was funded by Takeda Pharmaceutical Company Limited. **Author contributions:** R.B., S.Matsud., A.N., and H.K. conceived and designed the experiments. R.B., S.Matsud., Y.A., R.Y., N.S., H.O., and S.I. performed the experiments and analyzed the data. M.D., Y.H., S.Matsum., and M.I. designed and synthesized TAK-418. T.A. performed the bioinformatic analyses. R.B., S.Matsud., and H.K. wrote the manuscript. **Competing interests:** The authors are present employees of Takeda Pharmaceutical Company Limited or were employees of Takeda Pharmaceutical Company Limited while engaged in this research. S.Matsud., Y.A., R.Y., N.S., H.O., S.I., Y.H., M.I., and H.K. are shareholders of Takeda Pharmaceutical Company Limited. M.D., Y.H., S.Matsum., and M.I are inventors on patents related to this work filed by Takeda Pharmaceutical Company Limited (no. WO2015/156417, filed 09 April 2015, published 15 October 2015; US9,487,511B2, filed 09 April 2015, published 15 October 2015; US10,414,761B2, filed 29 January 2018, published 14 June 2018). The authors declare that they have no other competing interests. **Data and materials availability:** All data needed to evaluate the conclusions in the paper are present in the paper and/or the Supplementary Materials. Coordinate data in the crystal structure analysis have been deposited in the Protein Data Bank (PDB ID: 7E0G). RNA-seq, ChIP-seq, and RRBS data have been deposited in the Gene Expression Omnibus (accession number: GSE165676).

Submitted 6 November 2019
Accepted 28 January 2021
Published 12 March 2021
10.1126/sciadv.aba1187

Citation: R. Baba, S. Matsuda, Y. Arakawa, R. Yamada, N. Suzuki, T. Ando, H. Oki, S. Igaki, M. Daini, Y. Hattori, S. Matsumoto, M. Ito, A. Nakatani, H. Kimura, LSD1 enzyme inhibitor TAK-418 unlocks aberrant epigenetic machinery and improves autism symptoms in neurodevelopmental disorder models. *Sci. Adv.* **7**, eaba1187 (2021).

Science Advances

LSD1 enzyme inhibitor TAK-418 unlocks aberrant epigenetic machinery and improves autism symptoms in neurodevelopmental disorder models

Rina Baba, Satoru Matsuda, Yuuichi Arakawa, Ryuji Yamada, Noriko Suzuki, Tatsuya Ando, Hideyuki Oki, Shigeru Igaki, Masaki Daini, Yasushi Hattori, Shigemitsu Matsumoto, Mitsuhiro Ito, Atsushi Nakatani and Haruhide Kimura

Sci Adv **7** (11), eaba1187.
DOI: 10.1126/sciadv.aba1187